Metadata of the chapter that will be visualized online

Author	Family Name	**Wainwright**
	Particle	
	Given Name	**John**
	Suffix	
	Division	Department of Geography
	Organization	Durham University, Science Laboratories
	Address	DH1 3LE, Durham, UK
	Email	john.wainwright@durham.ac.uk
Author	Family Name	**Scarsoglio**
	Particle	
	Given Name	**Stefania**
	Suffix	
	Division	Dipartimento di Idraulica, Trasporti ed Infrastrutture Civili
	Organization	University of Turin
	Address	10129, Torino, Italy
	Email	stefania.scarsoglio@polito.it
Author	Family Name	**Tietjen**
	Particle	
	Given Name	**Britta**
	Suffix	
	Division	Institute of Biology
	Organization	Freie Universität Berlin
	Address	14195, Berlin, Germany
	Email	britta.tietjen@fu-berlin.de
Author	Family Name	**Jeltsch**
	Particle	
	Given Name	**Florian**
	Suffix	
	Division	Plant Ecology and Nature Conservation
	Organization	University of Potsdam
	Address	14469, Potsdam, Germany
	Email	jeltsch@uni-potsdam.de
Author	Family Name	**Mueller**
	Particle	
	Given Name	**Eva Nora**
	Suffix	
	Division	Institute of Earth and Environmental Science
	Organization	University of Potsdam

Address	14476, Potsdam, Germany
Email	eva.mueller@uni-potsdam.de

Abstract	Drivers of land degradation often co-occur and their effects are often non-additive because of internal system feedbacks. Therefore, to understand how drivers of land degradation alter ecogeomorphic patterns and processes, novel tools are required. In this chapter we explore different modelling approaches that have been developed to simulate pattern formation, ecological and geomorphic processes. These modelling approaches reflect some of the best available tools at present, but notably, they tend to simulate only one or at best two components of the ecogeomorphic system. The chapter culminates with a discussion of these different modelling approaches and how they provide a foundation upon which to develop much needed ecogeomorphic modelling tools.

Chapter 7
Approaches to Modelling Ecogeomorphic Systems

Laura Turnbull, Tamara Hochstrasser, Mareike Wieczorek, Andreas Baas, John Wainwright, Stefania Scarsoglio, Britta Tietjen, Florian Jeltsch, and Eva Nora Mueller

Abstract Drivers of land degradation often co-occur and their effects are often non-additive because of internal system feedbacks. Therefore, to understand how drivers of land degradation alter ecogeomorphic patterns and processes, novel tools are required. In this chapter we explore different modelling approaches that have been developed to simulate pattern formation, ecological and geomorphic processes. These modelling approaches reflect some of the best available tools at present, but notably, they tend to simulate only one or at best two components of the ecogeomorphic system. The chapter culminates with a discussion of these different modelling approaches and how they provide a foundation upon which to develop much needed ecogeomorphic modelling tools.

L. Turnbull (✉)
Institute of Hazards, Risk and Resilience, Department of Geography, Durham University,
Science Laboratories, DH1 3LE Durham, UK
e-mail: laura.turnbull@durham.ac.uk

T. Hochstrasser
School of Biology and Environment Science, Agriculture & Food Science Centre,
University College Dublin, Belfield, Dublin 4, Ireland
e-mail: tamara.hochstrasser@ucd.ie

M. Wieczorek
Alfred Wegener Institute for Polar and Marine Research, 14473 Potsdam, Germany
e-mail: mareike.wieczorek@awi.de

A. Baas
Department of Geography, King's College London, WC2R 2LS London, UK
e-mail: andreas.baas@kcl.ac.uk

J. Wainwright
Department of Geography, Durham University, Science Laboratories, DH1 3LE Durham, UK
e-mail: john.wainwright@durham.ac.uk

AQ1

AQ2

7.1 Why Model Ecogeomorphic Processes?

Land degradation in drylands is a complex phenomenon involving changes in pattern-process relationships. There are multiple drivers of land degradation in drylands which often co-occur. These include grazing, fire management, soil-surface disturbance, temperature change and precipitation change. To investigate how drivers affect pattern-process relationships, a widely used approach is single-factor experiments where one driver is experimentally manipulated at a time. However, multiple drivers co-occurring can each affect different biotic and abiotic components of the system. For instance, grazing can cause a direct reduction in biomass of forgeable plants, while other types of soil-surface disturbances can alter soil infiltrability and erodibility. Due to pattern-process and biotic-abiotic feedbacks that are inherent in drylands, the effects of co-occurring drivers tend not to be additive, thus introducing non-linear behaviour (Peters and Havstad 2006; Turnbull et al. 2008; Okin et al. 2009). Multi-factorial experiments, which enable the systematic exploration of multiple different drivers on system response, have become more widely used in ecological studies (for example Norby and Luo 2004) to tease apart the effects of different drivers. However, these experiments can become very large, especially when they are replicated. As a result, this type of experimental design tends to be favoured more by ecologists who tend to carry out investigations with greater ease at the plant-patch scale. Because multi-factorial experiments tend to be limited to small plots and a limited range of environmental conditions, extrapolating results to broader spatial scales is challenging. Multi-factorial experiments are much less widely used in geomorphic studies, because the larger spatial (and often temporal) scale of enquiry makes the implementation of replicated multi-factorial experiments virtually impossible. Since we are concerned here with understanding ecogeomorphic processes, the use of multi-factorial experimental designs has limited scope. New tools are needed to enable us to explore how drivers of land degradation affect ecogeomorphic processes across multiple spatial and temporal scales. The development of ecogeomorphic models has great potential to provide a new generation of tools that will enable us

S. Scarsoglio
Dipartimento di Idraulica, Trasporti ed Infrastrutture Civili, University of Turin,
10129 Torino, Italy
e-mail: stefania.scarsoglio@polito.it

B. Tietjen
Institute of Biology, Freie Universität Berlin, 14195 Berlin, Germany
e-mail: britta.tietjen@fu-berlin.de

F. Jeltsch
Plant Ecology and Nature Conservation, University of Potsdam, 14469 Potsdam, Germany
e-mail: jeltsch@uni-potsdam.de

E.N. Mueller
Institute of Earth and Environmental Science, University of Potsdam, 14476 Potsdam, Germany
e-mail: eva.mueller@uni-potsdam.de

to explore in greater depth the effects of co-occurring drivers on pattern-process 47
relationships in drylands and thus the dynamics of land degradation. For instance, 48
ecogeomorphic models will allow us to carry out modelling-based multi-factorial 49
experiments for different combinations of environmental drivers and disturbances, 50
initial conditions, parametric states and spatial scales; all of which cannot be 51
readily undertaken using field-based experimental approaches alone. To maximise 52
the development of ecogeomorphic modelling tools, both ecogeomorphic modelling 53
and ecogeomorphic field experimentation should be two-way; as well as using 54
modelling tools to guide the design field experimentation, modelling should also 55
be used as an tool to interpret results of field experimentation. 56

In developing ecogeomorphic modelling tools, perhaps the best starting place 57
is to outline the state-of-the-art modelling tools that have already been developed 58
to simulate biotic and abiotic patterns and processes in drylands. In this chapter, 59
deterministic and stochastic modelling approaches of pattern formation are detailed, 60
which are widely used in studies of pattern formation in drylands. Then, process- 61
specific [ecological and geomorphic] modelling approaches are explored, including 62
finite difference and finite element approaches, and rule-based approaches such 63
as cellular automata (CA) models. The first of these models is EcoHyd which 64
simulates soil moisture and vegetation dynamics. Next, ECOTONE is outlined, 65
which is used to explore the effect of gap formation on vegetation dynamics. The 66
effects of spatially variable vegetation and soil properties on runoff and erosion 67
dynamics are then explored using MAHLERAN, which is an event-based runoff 68
and erosion model. Wind erosion-vegetation feedbacks are investigated using the 69
cellular automata model, DECAL. In the concluding section of this chapter these 70
modelling approaches are discussed in terms of how they can be used to provide a 71
foundation upon which to develop ecogeomorphic models. 72

7.2 Deterministic Models of Pattern Formation 73

Theories used to explain self-organizing vegetation patterns are often based on 74
deterministic symmetry-breaking instability as discussed in detail in Chap. 3. 75
Symmetry-breaking instability is a mechanism whereby the spatial dynamics of 76
vegetation, resulting from cooperative and inhibitory interactions occurring at 77
different spatial ranges, destabilize the homogenous state of the system in turn 78
leading to heterogeneous distributions of vegetation and thus, pattern formation 79
AQ3 (Borgogno et al. 2009). 80

As an example of the deterministic approach, the now-classic example of Lefever 81
and Lejeune (1997) is considered, who attempted to explain the origin of patterns 82
in Tiger Bush using a form of what Borgogno et al. (2009) define as a kernel-based 83
model (see Sect. 3.7). The basic form of the Lefever and Lejeune model is: 84

$$\frac{\partial V}{\partial t} = RC - M \tag{7.1}$$

where V is the vegetation growth, expressed at community level (so ignoring the effects of different species); R is a function representing the reproduction of the vegetation, C is a function representing competition and other interactions producing a limit to growth, and M is a function reflecting vegetation mortality, either by autogenic or allogenic (e.g. fire, grazing) processes. The dynamics of the vegetation community are evaluated as $V(\mathbf{s}, t)$ where $\mathbf{s}$ is a point in space and t is time. Each of the functions R, C and M are defined as operating in the neighbourhood of the vegetation under consideration, with the neighbouring area defined as $\mathbf{s} + \mathbf{s}'$, based on weighting functions $w_{\{R,C,M\}} = w_{\{R,C,M\}} (\mathbf{s}', L_{\{R,C,M\}})$. The parameters $L_{\{R,C,M\}}$ are characteristic lengths over which the reproduction, competition and mortality interactions occur, which define the extent of spatial interactions in the model.

Lefever and Lejeune define the reproduction function as:

$$R = \int_\Omega \mathbf{d}\mathbf{s}' \lambda w_R \left(\mathbf{s}', L_R\right) V \left(\mathbf{s} + s', t\right) \left[1 + \mathcal{E} V \left(\mathbf{s} + s', t\right)\right] \tag{7.2}$$

where λ is the growth rate in the absence of interactions with other plants and $\mathcal{E}$ is a parameter reflecting the effects of cooperation on growth (e.g. through changes in local infiltration rate or nutrients through decay of shed parts). The competition function is:

$$C = 1 - \int_\Omega \mathbf{d}\mathbf{s}' w_C \left(s', L_C\right) \frac{V \left(\mathbf{s} + s', t\right)}{K} \tag{7.3}$$

where K is the maximal density of plants in a given area. The mortality function is:

$$M = \int_\Omega \mathbf{d}\mathbf{s}' \eta w_M \left(\mathbf{s}', L_M\right) V \left(\mathbf{s} + s', t\right) \tag{7.4}$$

where the mortality rate, η, is the inverse of the average lifespan of the vegetation. The model thus has seven parameters, three of which are measureable properties of the vegetation community. The weighting functions are taken to be Gaussian, so that in a 2D model:

$$w_i \left(\mathbf{s}', L_i\right) = \frac{1}{2\pi L_i^2} \mathbf{e}^{-\left(\frac{|s'|}{2L_i^2}\right)} \tag{7.5}$$

where $i = \{R,C,M\}$. Combining these equations and carrying out a linear stability analysis shows that symmetry-breaking instability can only occur to produce patterns when $L_R < L_C$, and when $K \mathcal{E} > 0$. In other words, the two conditions correspond to (i) the length scale over which reproduction occurs being shorter than the length scale over which competition occurs and the; and (ii) reproduction having to be cooperative, respectively. Defining the parameter $\mu = \eta/\lambda$, the stability analysis shows that patterns only occur at intermediate values $\mu_c \leq \mu \leq \mu'_c$. Lefever
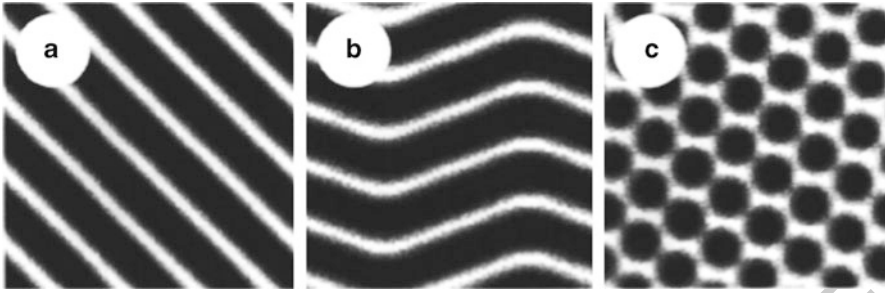
Fig. 7.1 Three examples of spatial patterns obtained for an isotropic system (*white regions* correspond to less-vegetated areas). (**a**) Pattern constituted of stripes having a uniform orientation ($\mu = 0.95$, $L = 0.1$, $\Lambda = 1$). The latter is determined by the initial condition. (**b**) Coexistence of stripes with two different orientations ($\mu = 0.95$, $L = 0.15$, $\Lambda = 1$). The relative orientation is determined by the choice of the parameters. The global orientation depends on the initial condition. (**c**) High-density *spots* arranged in hexagonal lattice on a low-density background ($\mu = 0.95$, $L = 0.1$, $\Lambda = 0.8$). In all cases, the periodicity corresponds to a wavelength approximately given by $\lambda_c = 2\pi/k_c$ (Source: Lefever and Lejeune 1997)

and Lejeune thus call μ a "switching parameter", and note that its value as the ratio of mortality to birth rates can also be considered as an index of aridity. Numerical simulation shows that the model can produce both striped and spotted patterns when the system is isotropic (i.e. not driven by fluvial or aeolian processes with a dominant direction: Fig. 7.1), and bands and arcuate features where there is anisotropy (Fig. 7.2). Key characteristics of the model are that the wavelength of the patterns decreases with vegetation density, that dynamic patterns under anisotropy can occur both in slope- and contour-parallel directions, and that contour-parallel bands tend to move upslope. All of these characteristics have been observed in Tiger Bush in the field (but see further discussions in Chaps. 12 and 13).

7.3 Basic Stochastic Processes Able to Induce Ordered Structures

The formation of vegetation patterns in drylands is commonly associated with symmetry-breaking instability in deterministic models, as outlined above. However, random fluctuations in environmental drivers may also play a critical role in the dynamics of patterns in non-linear systems (Borgogno et al. 2009; see also the discussion in Chap. 3). The emergence of new ordered states in dynamical systems, in time and in space, has been attributed to stochastic fluctuations – termed "noise-induced phase transitions" – which destabilize a homogeneous (symmetrical) state of the system (Scarsoglio et al. 2009). While random fluctuations in environmental processes are pervasive, applications of the theories of noise-induced pattern formation are rare and have only been developed more recently (Borgogno et al. 2009; Scarsoglio et al. 2009).
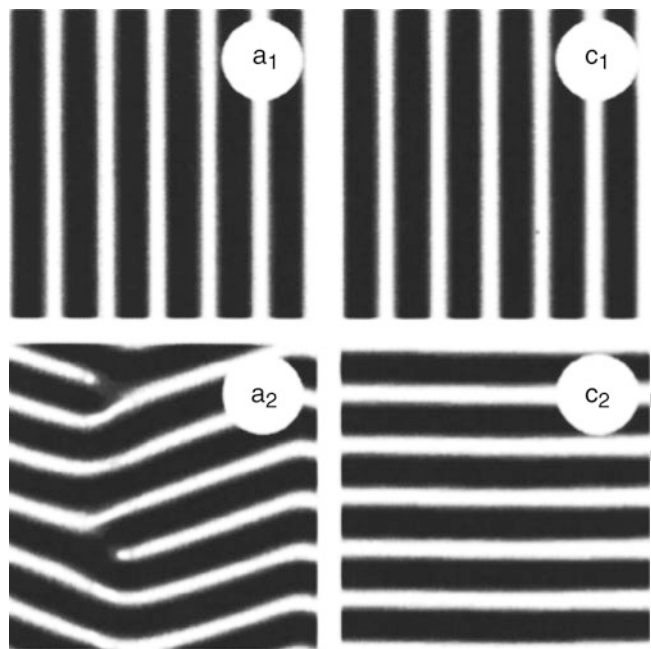
Fig. 7.2 Vegetation patterns in the anisotropic case. The influence of anisotropy (in the y direction) on reproduction (patterns a_1, c_1 obtained for $t_1 = 1$ and $t_2 = 0$) and on inhibition (patterns a_2, c_2 obtained for $t_1 = 0$ and $t_2 = 1$) is simulated. The simulations a_i ($i = 1,2$) correspond ($\mu = 0.95$, $L = 0.1$, $\Lambda = 1$), in the isotropic case, to a banded pattern (cf. Fig. 7.1a). The simulations c_i correspond ($\mu = 0.95$, $L = 0.1$, $\Lambda = 0.8$), in the isotropic case, to a pattern of hexagonal symmetry (cf. Fig. 7.1c). Reproduction anisotropy selects stripes parallel to the anisotropy direction and inhibition anisotropy selects stripes orthogonal to that direction, independently of the spatial symmetry properties of the patterns obtained in the isotropic case for the same values of parameters. Parallel stripes are static, while orthogonal stripes are moving upward, i.e. in the positive y direction (Source: Lefever and Lejeune 1997)

In order to explain the mechanisms of noise-induced pattern formation, two examples of stochastic models are outlined, which can be expressed by Eq. 3.11 presented in Sect. 3.8. The first model is:

$$\frac{\partial \phi}{\partial t} = -\phi + \xi\left(\overrightarrow{r}, t\right) + D\nabla^2 \phi. \tag{7.6}$$

where ϕ is vegetation cover. In this case, deterministic dynamics ($\xi\left(\overrightarrow{r}, t\right) = 0$) damp the field variable to zero and do not exhibit steady pattern formation. The additive noise ($\xi\left(\overrightarrow{r}, t\right) \neq 0$) is able to keep the system away from the homogeneous state, while the spatial coupling induces spatial coherence. Thus, pattern formation is clearly noise-induced and arises from a synergism between additive noise and spatial coupling.
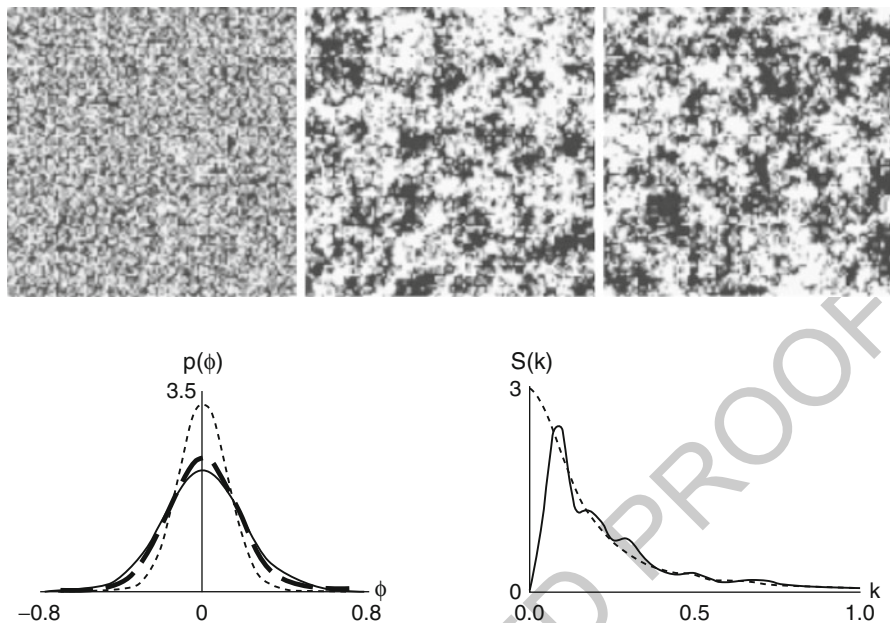
Fig. 7.3 Model (7.6.1) with $D = 50$, $s = 3$. *Top*: Numerical simulation of ϕ at $t = 0,10,100$. *Bottom*: pdf (*solid line*: numerical simulation; *dotted line*: classic mean-field analysis, *thick*: corrected mean-field analysis; Sagues et al. 2007) and azimuthal-averaged power spectrum S (*solid*: numerical simulations, *dotted*: structure function) of ϕ at $t = 100$. The numerical simulations use the Heun's scheme (Sagues et al. 2007) on a two-dimensional square lattice with 128×128 sites, with periodic boundary conditions, and uniformly distributed initial conditions between [−0.01, 0.01]. *Black* and *white tones* in the figures represent positive and negative values of the field, respectively, with *black* representing vegetation

Figure 7.3 shows the onset of patterns in the model (Eq. 7.6). No clear periodicity is visible but many wavelengths are present to produce multiscale patterns with irregular boundaries, which persist in the steady state. No phase transition occurs since the probability density function (pdf), which is numerically and analytically determined at steady state (see Chap. 3 for more detail), remains unimodal and with zero mean.

Numerical and analytical results in the Fourier space (see Sect. 8.4.4.2) confirm that there is no dominant wavelength different from zero. Equation 7.6 can be used to express the temporal evolution of the existing vegetation, ϕ, as the result of a local linear decreasing dynamics, random rainwater availability, and vegetation's ability to develop spatial interactions. The distribution of vegetated sites in semi-arid environments exhibits spatial configurations resembling those shown in Fig. 7.3 (von Hardenberg et al. 2010; Scanlon et al. 2007).

The second model is:

$$\frac{\partial \phi}{\partial t} = -\phi - \phi^3 + \phi \xi \left(\overrightarrow{r}, t \right) - D \left(\nabla^2 + k_0^2 \right)^2 \phi \tag{7.7}$$
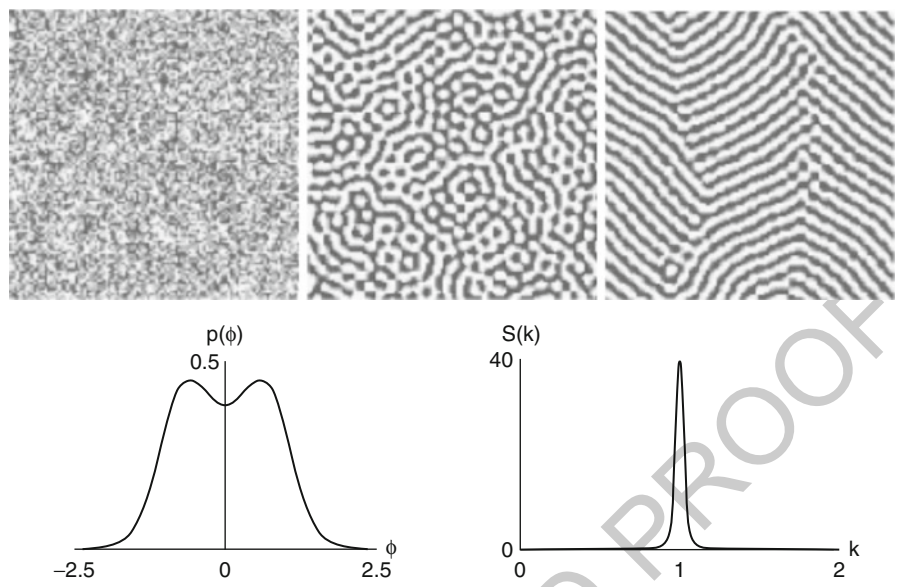
AQ4

Fig. 7.4 Simulation results of the model represented by Eq. 7.7.2 with $D = 20$, $s = 2$, $k_0 = 1$. *Top*: numerical simulation of ϕ at $t = 0$, 10, 100. *Bottom*: pdf and azimuthal-averaged power spectrum S of ϕ at $t = 100$. See Fig. 7.3 for details on the numerical simulation

In this case, pattern formation relies on two actions: (i) multiplicative noise $(\phi\xi\left(\overrightarrow{r}, t\right))$ temporarily destabilizes the dynamics, and (ii) spatial coupling exploits this short-term instability, giving rise to the pattern. If the noise intensity is below a critical threshold ($s < s_c$) or if the noise is absent ($\xi\left(\overrightarrow{r}, t\right) = 0$), patterns are transient and fade away as the system approaches steady state. If the noise intensity exceeds the threshold ($s > s_c$), steady patterns occur.

Figure 7.4 displays an example ($s > s_c = 1$) where patterns exhibit a clear dominant wavelength and are statistically stable, although in the transient they evolve from a labyrinthine to a striped shape. At $t = 100$, the pdf of the field shows a weak bimodality with zero mean, demonstrating that no phase transition occurs, while the power spectrum has a peak corresponding to k_0, confirming that a clear periodicity is present. Equation (7.7) can be used to describe the temporal evolution of vegetation, ϕ, as the result of a local biomass loss, a disturbed local increasing dynamics, and the interplay between long and short-range interactions. A number of environmental patterns exhibit a regular and periodic spatial behaviour similar to the one shown in Fig. 7.4 (Couteron and Lejeune 2001; Lefever et al. 2009). Remarkable examples are given by peatlands (Eppinga et al. 2008), arctic hummocks and patterned ground (Gleason et al. 1986), and vegetation in semi-arid regions (e.g. Valentin et al. 1999; Esteban and Fairen 2006; Ridolfi et al. 2011).

Although this stochastic modelling approach and the deterministic modelling approach outlined previously are both able to reproduce patterns, they do not

AQ5

contribute to understanding the physical mechanisms that are responsible for pattern formation. In the following sections, models that attempt to address these mechanisms more directly will be considered.

7.4 Modelling Feedback Mechanisms Between Vegetation, Soil-Moisture Dynamics and Degradation

The model EcoHyD (Tietjen et al. 2010) is a combination of a two-layer soil-moisture-dynamics model, HydroVeg (Tietjen et al. 2009), and a dynamic vegetation model, which has been used previously to explore the effects of intra-annual rainfall variability and temperature on coupled water-vegetation dynamics in drylands (Tietjen et al. 2010; Jeltsch et al. 2010c). This modelling approach enables the effects of hydrological and ecological processes and their feedbacks to be disentangled. EcoHyD is spatially explicit and grid-based. Each cell has a spatial resolution of 5×5 m and is characterized by a specific topographic height. The spatial extent of the model domain is adjustable. Open boundary conditions are implemented so that water losses due to runoff are possible. Hydrological processes are simulated on an hourly to daily resolution and ecological processes on a fortnightly to yearly basis. The main processes represented in EcoHyd are presented in Fig. 7.5.

In HydroVeg, precipitation is received at hourly intervals and accumulates on the surface and infiltrates into soil layers, either as fast infiltration into deeper layers along roots and via macropores or slower infiltration into the upper layer according to the Green and Ampt (1911) approach. If the amount of surface water exceeds the hydraulic conductivity of the soil, ponding occurs and surface water is lost to the lowest neighbouring cell. Further water losses from a cell occur as evapotranspiration (ET) which is calculated daily using the Hargreaves (1974) approach. Between the two soil layers, a diffusive flux is accounted for, as well as water loss to deeper layers by drainage. Infiltration, runoff and water loss by ET depend on soil texture and the prevailing vegetation cover. The amount of surface water runoff per hour is furthermore dependent on the slope of a cell and increases with steepness (following the approach of Manning-Strickler: Dingman 1994).

EcoHyd simulates the fate of two vegetation-growth forms: grasses and shrubs/trees, which are the main life forms in the simulated savannas. Plants compete for water and space, and vegetation cover changes as a result of water-dependent growth, mortality and dispersal. Fortnightly growth follows a logistic behaviour and is reduced by limited water availability and competition. Mortality results from low soil-moisture content during the growing season, or direct removal of vegetation due to disturbances such as grazing. Grass dispersal is assumed to be homogenous in space, while shrub dispersal is limited and decreases exponentially with distance from the source cell. Both mortality and dispersal are calculated yearly, at the end of the growing season.
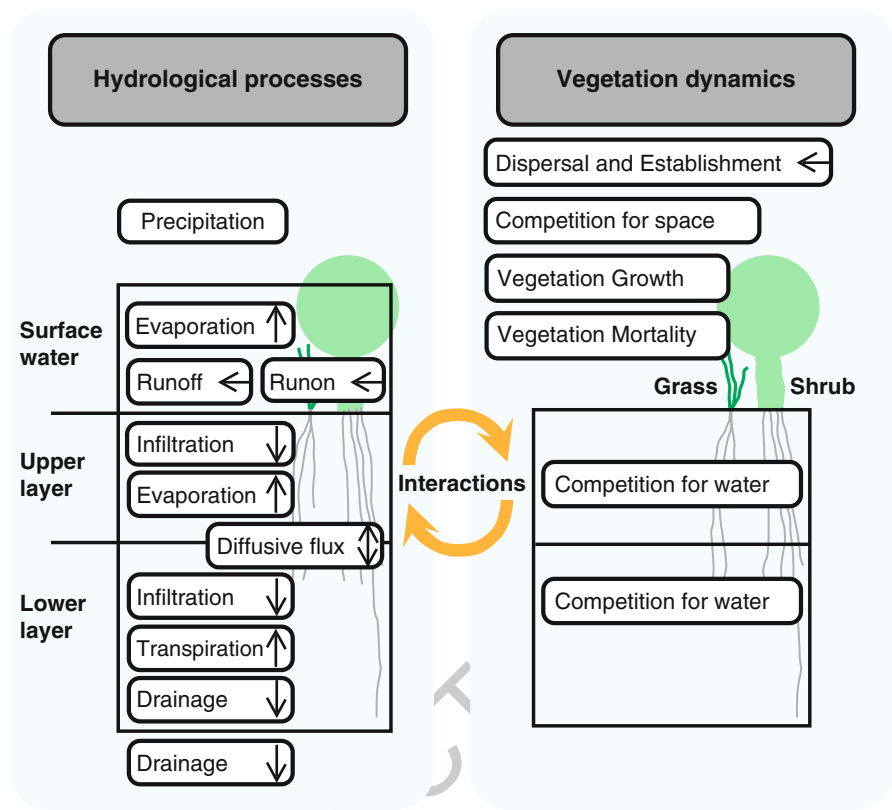
Fig. 7.5 Overview showing the main components of EcoHdy: HydroVeg (*left*) and the dynamic vegetation model (*right*). Processes represented within a single grid cell and interactions between cells are shown (Adapted from Tietjen et al. 2010). *Arrows* indicate the direction of interactions between cells and soil compartments (↓: water reaching compartment; ↑: water leaving compartment; ←: water/seed exchange between cells)

Exploratory analysis is first carried out using only HydroVeg (Tietjen et al. 2009) to determine the effects of static vegetation cover, vegetation composition and soil texture on soil moisture dynamics for a single precipitation event on a flat site. Longer term feedbacks to growth, mortality and dispersal are not considered in this instance, but are addressed in subsequent exploratory analysis using EcoHyd. In these initial simulations, total soil depth was set to 0.80 m, with the top 0.20 m belonging to the upper soil layer (following Tietjen et al. 2010). The effects of differences in vegetation cover (grass and shrub) on soil moisture for a 15 mm precipitation event, distributed within 1 day followed by 11 dry days are presented in Fig. 7.6. Results show that moisture dynamics in the upper soil layer are hardly impacted by vegetation composition or soil texture, since the flat topography leads to negligible runoff of surface water and therefore most water eventually infiltrates. In contrast both vegetation composition and soil texture influence soil-moisture
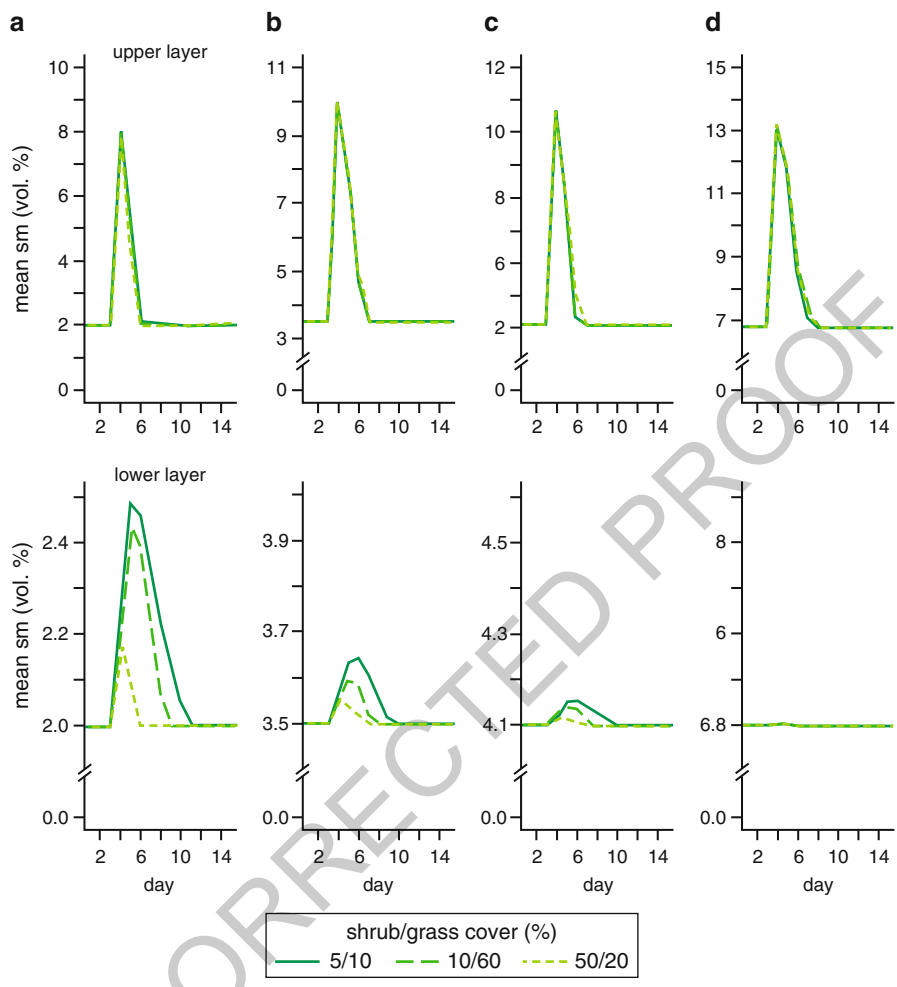
Fig. 7.6 Soil moisture (*sm*) after a 15 mm precipitation event, for two soil layers (*upper and lower panel*), three vegetation covers and four soil types (**a**) sand, (**b**) loamy sand, (**c**) sandy loam and (**d**) sandy clay loam

dynamics in the lower layer. Infiltration depth is strongly determined by soil texture. Fine textured soils do not facilitate much deep infiltration, whereas coarse textured sandy soils do. Therefore coarse textured sandy soils may create favourable conditions for shrubs, potentially leading to higher encroachment on sandy than on loamy soils. Vegetation composition has a strong impact on soil-moisture dynamics in the lower soil layer. A higher shrub cover rapidly reduces soil moisture in the lower soil layer after a precipitation event via transpiration within 2 days. In contrast, with higher grass cover it takes up to 5 days until soil moisture is reduced down to the residual water content.
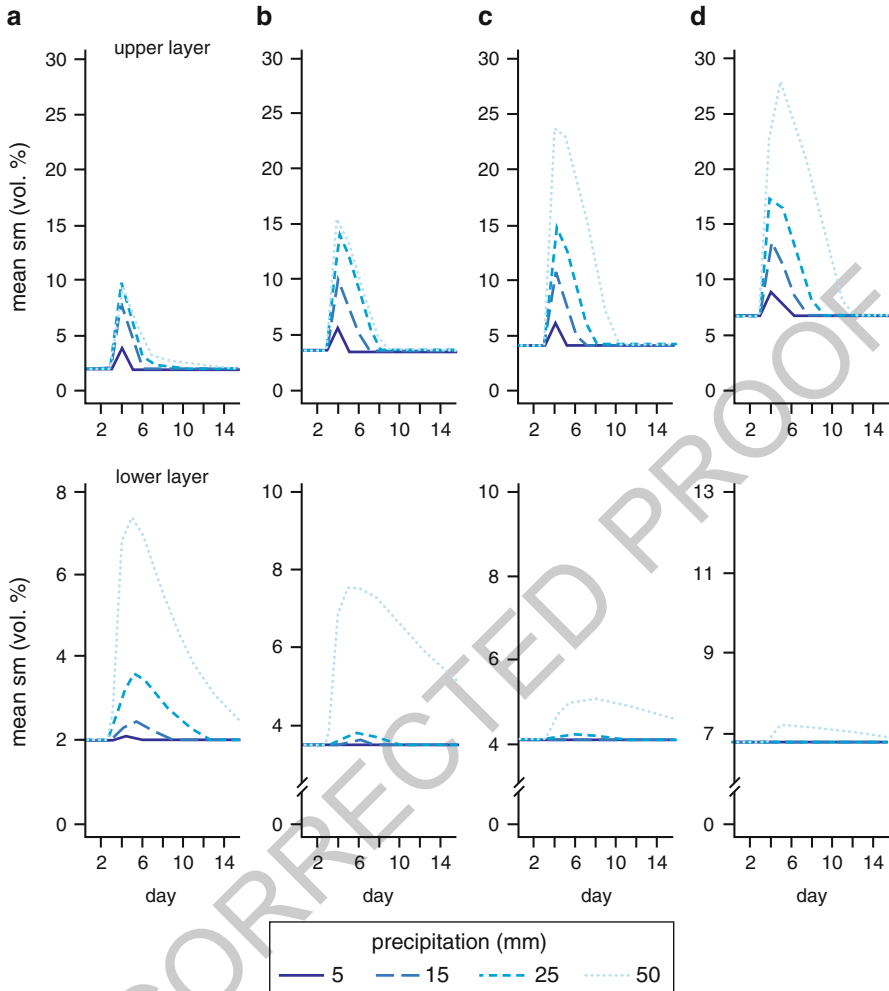
Fig. 7.7 Soil moisture (*sm*) after four different precipitation events (5, 15, 25 and 50 mm) for two soil layers (*upper and lower panel*) and four soil types (**a**) sand, (**b**) loamy sand, (**c**) sandy loam and (**d**) sandy clay loam with 60 % grass cover and 10 % shrub cover

To assess the impact of extreme events, soil-moisture dynamics were examined 243
after single precipitation events of different intensities (totals of 5, 15, 25, and 244
50 mm on 1 day), followed by 11 dry days (Fig. 7.7) in simulations with 10 % 245
shrub cover and 60 % grass cover. The results demonstrate that a shift to more 246
extreme events as predicted in the course of climate (Easterling et al. 2000) will 247
influence water availability for plants in shallow and deeper soil layers differently 248
for different soil textures. While soil texture mainly influences the lower soil layer 249
for smaller events as shown above, high intensities of precipitation additionally 250

influence soil moisture in the upper layer with highest changes of the water content 251
in fine textured soils. Although topography and runoff were not accounted for in 252
this analysis, spatial variations in soil texture in topographically variable landscapes 253
influences water losses further, by affecting runoff generation which is higher on 254
soils with low permeability and sites with low vegetation cover (Martinez-Mena 255
et al. 1998; Bartley et al. 2006). 256

In a further analysis using EcoHyd, feedbacks between vegetation and soil 257
moisture are explored in the case of Namibian savannas. Four major soil-texture 258
classes can be found in Namibia, namely sand, loamy sand, sandy loam and sandy 259
clay loam (Schwartz 2006). Mean annual precipitation ranges from less than 50 mm 260
to more than 600 mm (Atlas of Namibia Project 2002). Livestock farming plays a 261
prominent role in Namibian agriculture (Ministry of Agriculture, Water and Forestry 262
2009). However, high grazing pressure can lead to either shrub encroachment or 263
to a reduction in vegetation (Rietkerk and Van de Koppel 1997; Roques et al. 264
2001; Kuiper and Meadows 2002). This degradation is thought to be enhanced by 265
climate change (Fischlin et al. 2007). In Jeltsch et al. (2010b) EcoHyD was used 266
systematically to assess the impact of different combinations of climate change, 267
soil type and grazing intensity on savanna degradation for a broad range of semi- 268
arid Namibian savanna sites. In this analysis, EcoHyD was applied to four different 269
soil textures and three precipitation regimes, spanning the extent of the Namibian 270
thornbush savanna (Joubert et al. 2008), with mean annual precipitation (MAP) 271
ranging from 200 to 500 mm (Fig. 7.8). 272

Grazing by cattle was varied from low to high intensity, represented as annual 273
grazing rates of 2, 5, 10 and 20 % of the grass cover. To allow for better comparison, 274
the same topography was applied to all areas in the model. The effects of climate 275
change were implemented by reducing mean annual precipitation of each site by 276
10 % and increasing mean annual temperature by 2.25 °C, following Jeltsch et al. 277
(2010b). An index *deg* (Jeltsch et al. 2010c) was developed to reflect possible 278
vegetation changes and degradation trends and describes the change of perennial 279
grass cover as a consequence of grazing in comparison to scenarios without grazing 280
(deg = cover perennial grasses). If the absolute value and mean increase of shrub 281
cover after 30 years is higher than 5 %, the absolute value of deg (namely |deg|), 282
is multiplied by (+1), else it is multiplied by (−1). Since all scenarios in our 283
simulations show a negative trend of grass cover under grazing, i.e. deg < 0, high 284
negative values indicate a prominent risk of desertification by vegetation losses, 285
while positive values indicate potential shrub encroachment. 286

Simulation results show an increasing risk of vegetation degradation with 287
increasing grazing intensity (Fig. 7.8): grass cover decreases (quantity given by 288
the size of the bars), while the change in shrub cover (sign of *deg*) depends on the 289
combination of grazing intensity, precipitation, soil texture and the climate scenario. 290
None of the scenarios show shrub encroachment under low grazing intensity, 291
since grass still dominates the system. However, if grazing reduces grass cover 292
substantially by 5 % or more, shrub encroachment can occur, depending on soil 293
texture and MAP. With finer the soil texture, fewer scenarios lead to an increase 294
of woody vegetation. If the same grazing scenario is applied under climate-change 295
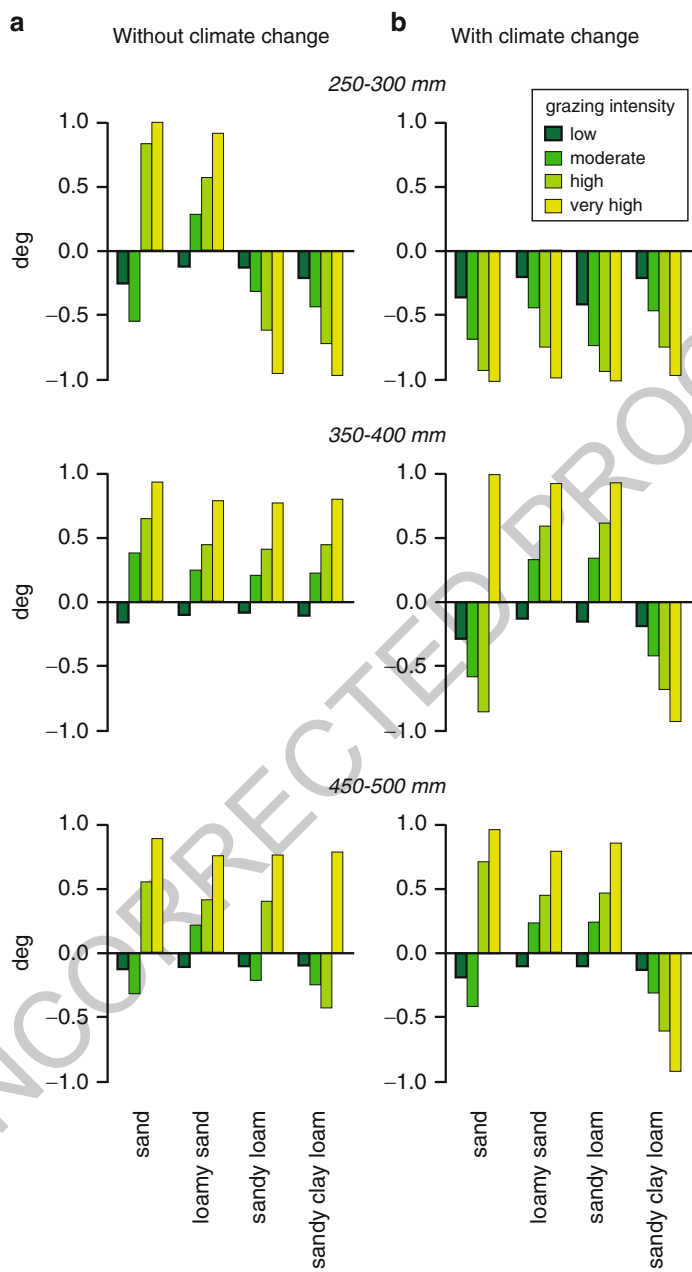
Fig. 7.8 Effects of 30 years of grazing with different intensities on the risk of savanna degradation without (**a**) and with (**b**) climate change (cc). Savanna areas are categorized according to actual mean annual precipitation (250–300, 350–400 and 450–500 mm). Degradation risks are summarized with an index *deg*, which integrates information on loss of perennial grass cover and risks of shrub encroachment (positive values indicating shrub encroachment versus negative values indicating desertification, see text for further details)

scenarios, the predicted increase of shrub cover is reversed for the two drier sites, 296
since the low soil-moisture content does not sustain dense vegetation cover. In 297
contrast, under more moist conditions shrub encroachment is still possible. Little 298
water infiltrates into the deep soil layers of sandy clay-loam soils (Figs. 7.6 and 7.7). 299
At these sites, shrub encroachment does not occur under reduced precipitation and 300
increased temperature, even at high grazing intensities (see also Sala et al. 1997; 301
Dodd and Lauenroth 1997). These results show that soil texture plays a crucial role 302
in the response of vegetation to grazing. Furthermore, these results suggest that grass 303
cover suffers most from grazing and climate change on soils with a high fraction of 304
sand, which may be the result of the higher pore size distribution of sandy soils 305
(Rawls et al. 1982) which allows for more infiltration into deeper soil layers. Less 306
water is lost to evaporation from lower soil layers (Noy-Meir 1973) and is therefore 307
available for plants for a longer period (Fig s. 7.4.2 and 7.4.3), which may especially 308
benefits shrubs with their deep rooting system (Walker et al. 1981; Sala et al. 1997). 309

AQ6

7.5 Modelling Vegetation Dynamics Using Gap-Dynamics Models
310
311

An alternative approach to simulate vegetation dynamics is to use gap-dynamics 312
models. Gap formation is a key process in the dynamics of plant communities (Li 313
et al. 2005). Gaps provide opportunities for the regeneration of resident plant species 314
and also for the establishment of newcomers. Therefore gaps are thought to play 315
a major part in regulating species composition and plant diversity (Grubb 1977; 316
Silvertown and Smith 1988; Li et al. 2005). Gap models simulate the establishment, 317
growth and mortality of each individual plant on a small plot (Coffin and Urban 318
1993; Bugmann 2001; Perry and Enright 2006), and have become one of the 319
most-used approaches for modelling vegetation dynamics. Gap models are based 320
on the principle of niche differentiation between different plant species, in terms 321
of their ability to compete for limiting resources (*competition*) and to cope with 322
environmental fluctuation and disturbance (*mortality* and *recruitment*). 323

ECOTONE is a gap-dynamics model developed for simulating vegetation dy- 324
namics of grasslands, invasive species and shrublands in arid and semi-arid areas 325
(Goslee et al. 2001; Peters 2002; Hochstrasser and Peters 2005; Goslee et al. 2006). 326
ECOTONE simulates vegetation dynamics on small plots, which are equivalent 327
to the size of a full-grown individual of the dominant plant. Vegetation dynamics 328
consist of a micro-succession of individuals from different functional groups or 329
plant species, which is induced by the mortality of plants (i.e. the opening of 330
resource gaps) (Fig. 7.9). In ECOTONE, plants compete for water (the most limiting 331
resource in drylands) during this micro-succession. The distribution of available 332
water is simulated using the soil-water model, SOILWAT (SOILWAT, Parton 1978). 333
Water dynamics are calculated on a daily time step, while competition for available 334
water occurs on a monthly basis, and growth and mortality of plants on a yearly 335
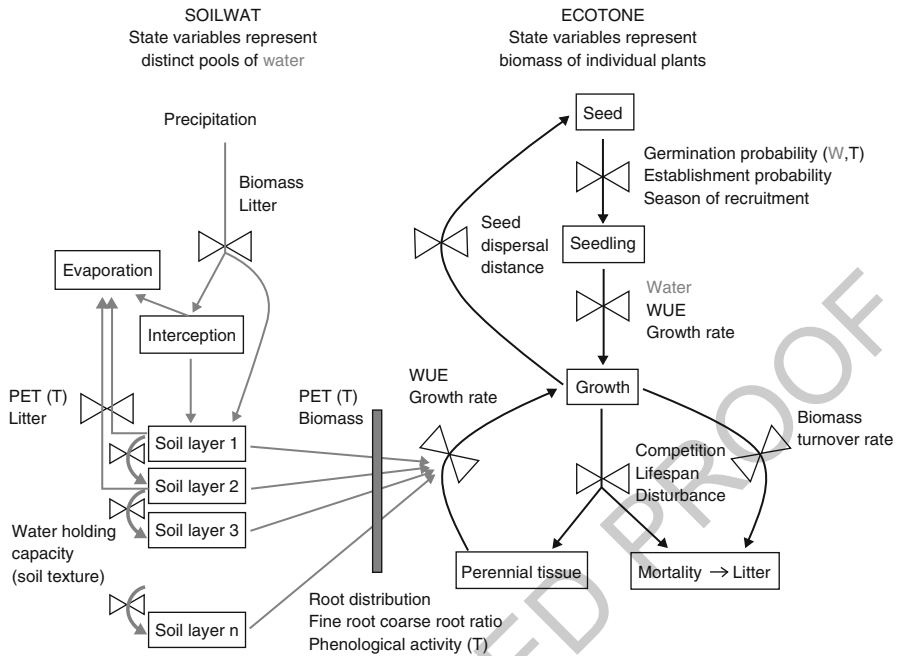
Fig. 7.9 Flow diagram of ECOTONE. *Grey arrows* indicate flows of water, *black arrows* indicate flows of biomass. Available water for plant growth depends both on climate (precipitation, temperature, PET) as well as on species characteristics (bar between SOILWAT and ECOTONE). *Letters in parentheses* after control variables indicate if they are dependent on water (*W*) or temperature (*T*) (Source: Hochstrasser 2001)

basis. The differences between these temporal resolutions of processes in the model were necessary since water dynamics can only be accurately simulated with high temporal resolution (Parton et al. 1998), whereas low temporal resolution is sufficient for simulating vegetation dynamics (Peters 2002).

Vegetation dynamics are driven by plant mortality, which opens up resource space (Fig. 7.9). Plants die due to competition, age, turnover and disturbance (Peters 2002). For example, young plants are less competitive than older plants because of their small size, while mortality increases with plant age, and therefore affects larger individuals (Coffin and Urban 1993; Bugmann 2001). Mortality may also occur due to competition and disturbance. Plant recruitment is determined stochastically, based on species recruitment probability, which is determined by seed availability multiplied by establishment probability (Peters 2002). It has been shown that recruitment can also be made a function of abiotic conditions, assuming that propagules are present in the soil (Hochstrasser 2001).

The ability of plants to acquire resources is strongly dependent on their biomass, especially leaf area for photosynthesis and root surface area for water uptake. In ECOTONE growth of plants is determined by symmetric competition for water

between individual plants on the same plot. The amount of water taken up by each 353
plant depends on its root biomass in each soil layer and its phenological activity 354
(Peters 2002). An alternative approach (Hochstrasser 2001) uses asymmetric com- 355
petition – i.e. larger plants are able to take up disproportionately more resources 356
than they would based on the difference in biomass (Schwinning and Weiner 1998). 357
It is assumed that all plants can take up water within the same range of soil- 358
water potential, although there are limitations associated with this assumption. For 359
example, creosotebush (*Larrea tridentata*) may be able to draw water from the soil 360
at much lower water potentials than other arid land plants (Barbour et al. 1977). 361
Water-use efficiency (WUE) determines how much the plant can grow given the 362
water taken up. WUE can also be used to account indirectly for species-specific 363
ranges of available water (Hochstrasser 2001). 364

In the following application of ECOTONE, recovery dynamics of black grama 365
(*Bouteloua eriopoda*) grasslands versus mesquite (*Prosopis glandulosa*) shrublands 366
following vegetation disturbance by traffic are investigated, using ECOTONE 367
(Hochstrasser et al. 2005). ECOTONE was parameterized for black grama grass- 368
lands and mesquite shrublands in southern New Mexico. The model was driven by 369
80 years of daily weather data from the Jornada Experimental Range (1918–1997), 370
southern New Mexico. Nine species and subdominant functional groups were 371
simulated. Species parameters were derived from a literature survey of the dominant 372
species (Hochstrasser et al. 2002). For subdominant species, existing parameter- 373
izations of the model were used (e.g. Hochstrasser 2001; Peters 2002). Vegetation 374
composition was matched with field records of the vegetation on the soil used in this 375
model (Hochstrasser et al. 2005). Plot-size was determined according to the resource 376
space of a full-grown mesquite (1.0 m^2) and black grama plant (0.25 m^2). Dynamics 377
for black grama and mesquite were investigated separately because these two life- 378
forms operate at a different scale and this scale difference and its implications 379
for grass-shrub interactions cannot yet be simulated well within ECOTONE. The 380
overall objective of the study was to demonstrate how the difference in resistance 381
(i.e. to the amount of damage done to the plant by disturbance) and resilience (i.e. 382
the ability of the plant to recover from disturbance) between grasses and shrubs 383
affects their recovery dynamics after disturbance. The tolerance range for pressure 384
from disturbance was set highest for grasses, intermediate for shrubs and lowest for 385
forbs (Hochstrasser et al. 2005). 386

Disturbance from vehicular traffic was simulated by partial or full mortality 387
of the aboveground (and indirectly belowground) biomass of the plant. Effects of 388
the disturbance were investigated at two levels: (i) the individual plant level (for 389
disturbance intensities below the maximum tolerance of individual plants) and (ii) 390
the population level (for disturbance intensities above the maximum tolerance of 391
individual plants). 392

- A one-time disturbance was applied to an individual on a single plot to determine 393
  the effects of a using range of disturbance intensities, from a low pressure 394
  impact (one passage of foot traffic) to a high pressure impact just below the 395
  plant's maximum tolerance (one passage by a heavy vehicle). If the pressure 396
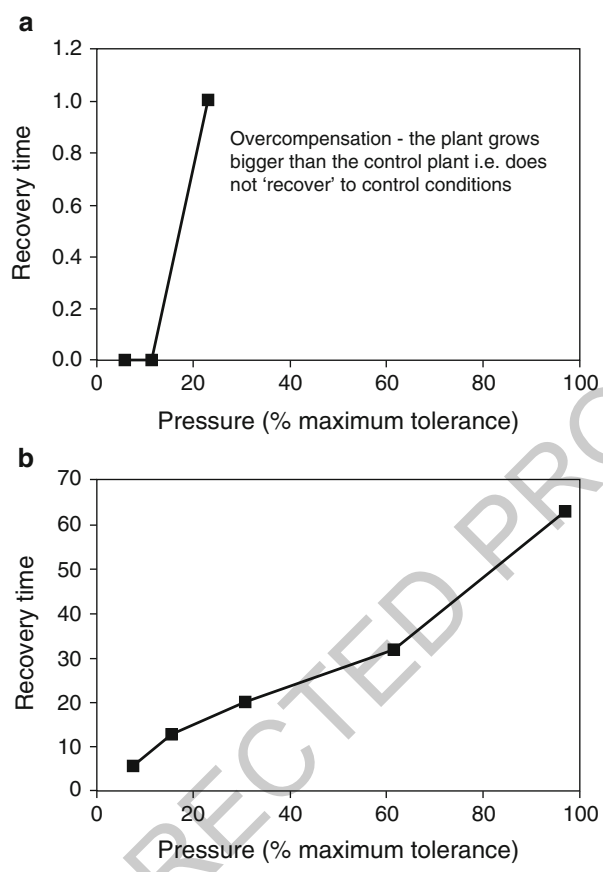
Fig. 7.10 Recovery of individual plants after a range of disturbances with different intensities. (**a**) Black grama (*Bouteloua eriopoda*) – a perennial grass with high tolerance of pressure – if the pressure applied was higher than 40 % of the maximum tolerance of plants, the impact of the disturbance on competitors of black grama resulted in the disturbed plant growing bigger than the control, thus not ever matching the control plants' biomass within 2 % (overcompensation). (**b**) Mesquite (*Prosopis glandulosa*) – a perennial shrub with low tolerance of pressure – recovery is slow in this case, but will occur – even at high pressures close to the tolerance range of the plant (Source: Hochstrasser et al. 2005)

impact was higher than the plant's tolerance, the plant died. When pressure 397 was below the maximum tolerance, plant-recovery time (defined as the time it 398 took the individual affected to get within 2 % of the aboveground weight of 399 a control plant for the same year) was significantly different for black grama 400 grass and a mesquite shrub (Fig. 7.10). Black grama recovered within a year 401 from low intensity disturbances and grew bigger than the control plant when 402 disturbance intensity was higher (but below maximum tolerance) (overcompen- 403

sation). The latter could be explained by the disturbance impact on competitors 404
of black grama, which allows the already dominant plant on the plot to capture 405
more resources than were previously available. In contrast, the recovery time of 406
a mesquite shrub increased with the disturbance intensity. At intensities close 407
to the shrub's maximum tolerance it takes up to 60 years to recover from the 408
disturbance. The differences in the recovery of these two species can be explained 409
by the amount of biomass removed by the disturbance as well as their growth rate. 410
Black grama loses less biomass during disturbance, and has a higher growth rate 411
than mesquite. 412

- At high intensities of disturbance – above the tolerance range of plants – the 413
recovery from disturbance depends on recruitment. The latter may depend on 414
the spatial extent of the disturbance. These effects were simulated indirectly by 415
incorporating the effects of reduced seed availability on recruitment. A vegetation 416
patch of 5×5 m in mesquite shrubland (25 plots) and 2.5×2.5 m (25 plots) in 417
black grama grassland was simulated. Model results show that the black grama 418
population was greatly reduced by the disturbance. Without dispersal limitation 419
after the disturbance, as may occur in a small disturbance patch, the black grama 420
population took an average of 20 years to recover. In contrast, the mesquite 421
population took longer to recover to the control level (on average about 50 422
years). In the control simulation, mesquite biomass started to decline after year 423
150 as the population reached its maximum lifespan of 200 years. In contrast, 424
the individuals in the disturbed populations were younger and maintained a 425
high level of biomass at the end of the simulation run. Dispersal limitation 426
after the disturbance, as may occur in large disturbance patches, impacted the 427
recovery dynamics of both dominants (Fig. 7.11): the black grama population 428
still recovered relatively rapidly, but could never attain the average biomass of 429
the plot without the dispersal limitation. These results indicate that black grama 430
populations are dependent on relatively high recruitment rates to maintain their 431
population size and thus despite their high resistance and resilience to disturbance 432
they are more vulnerable to disturbances than mesquite. In contrast, even though 433
recovery in the mesquite population was slower than in a non-dispersal-limited 434
situation, the population recovered and even expanded after the disturbance. 435

Results from this application of ECOTONE correspond with previous exper- 436
iments investigating the effects of trampling disturbance on different life forms 437
(Cole 1995; Yorks et al. 1997), demonstrating that the parameters used in gap- 438
dynamics models to differentiate species with regard to their ability to compete 439
for water, deal with environmental fluctuation and allogenic disturbance, can be 440
used to forecast the behaviour of these species, and thus vegetation dominance and 441
composition under different scenarios. While it is not possible to verify the accuracy 442
of model simulations due to a lack of long-term experiments on vegetation recovery 443
dynamics, these results provide valuable insight into plant-recovery dynamics and 444
variations between species. 445

a

b
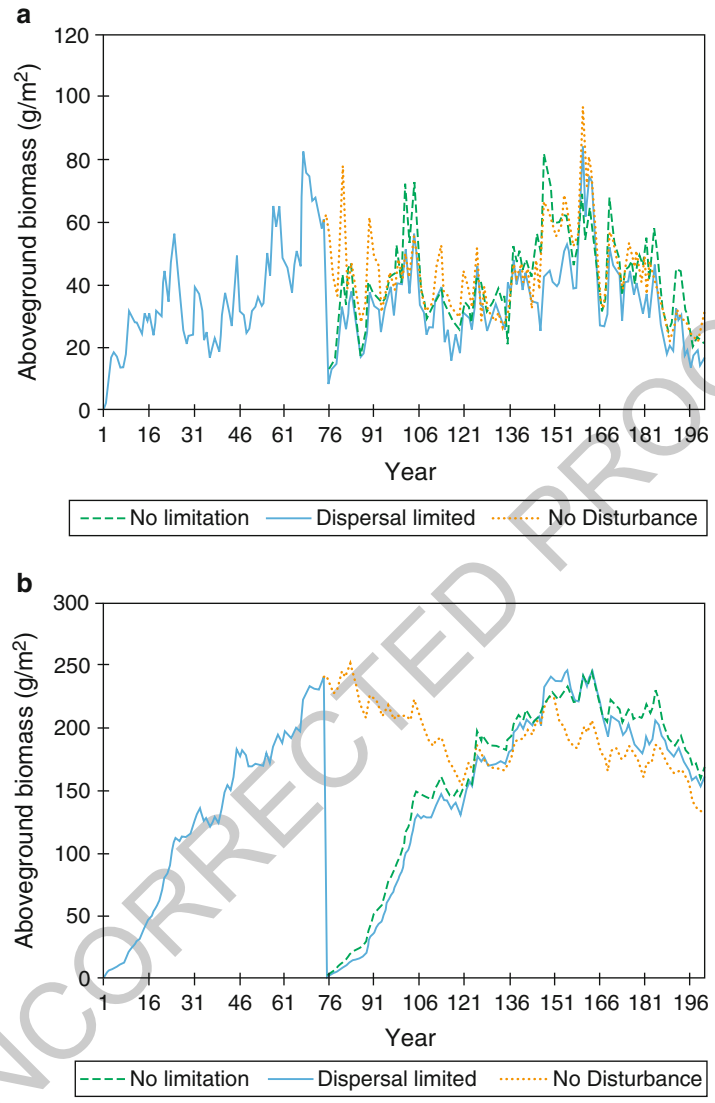
Fig. 7.11 Recovery of plant populations after high intensity disturbance (causing plant mortality). (**a**) Recovery of black grama (*Bouteloua eriopoda*) population is compared to (**b**) recovery of mesquite (*Prosopis glandulosa*) population. A situation with no dispersal limitation (as in a small disturbance) is compared to a dispersal limited situation (as in a large disturbance). The two cases are compared to a situation where no disturbance occurs to control for the natural variability of the vegetation (Modified from: Hochstrasser et al. 2005)

## 7.6 Modelling Redistribution of Water and Soil Resources 446

Spatial and temporal variation in vegetation and soil properties (discussed in 447
the previous two sections) as well as surface microtopography have a profound 448
influence on runoff and erosion (e.g. Wainwright et al. 2000; Abrahams and Parsons 449
1991; Calvo-Cases et al. 2003; Cammeraat 2004). The extent to which vegetation 450
patches are connected and orientated in relation to predominant flow lines and the 451
connectivity of soil properties and runoff-generating patches govern the runoff and 452
erosion response at broader spatial scales (Bracken and Croke 2007; Müller et al. 453
2007a; Turnbull et al. 2008, 2010). 454

In many drylands, runoff is typically generated by relatively short-duration high- 455
intensity rainfall events during which the infiltration capacity of the soil is often 456
exceeded, leading to the generation of infiltration-excess overland flow (Horton 457
1945; Wainwright and Bracken 2011) which is one of the primary vectors of 458
resource redistribution in drylands. 459

High-resolution timescales are necessary for modelling runoff and erosion in 460
drylands, and therefore such models tend to be event based. Distributed modelling 461
approaches are required because of the importance of the spatial distribution 462
of vegetation, soil characteristics, and microtopography on runoff and erosion 463
processes. Most spatially distributed modelling approaches divide the hillslope 464
or catchment into a grid, which allows the effects of patterns on process to be 465
represented. Water and soil resources are routed from cell to cell over the grid, using 466
one of a number of standard flow-routing algorithms. In a distributed representation 467
of a hillslope or catchment, each cell has a unique parameter value such that 468
spatial variability of surface properties is represented. The spatial and temporal 469
resolution of models simulating runoff and soil-redistribution processes is critical in 470
terms of representing adequately the heterogeneity of surface characteristics and the 471
temporal variability of rainfall characteristics, especially short bursts of especially 472
high-intensity rainfall (Wainwright and Parsons 2002). 473

An example of a high-resolution event-based runoff-erosion model is 474
MAHLERAN (Model for Assessing Hillslope to Landscape Erosion, Runoff And 475
Nutrients). MAHLERAN is made up of three primary submodels: the runoff 476
submodel, the erosion submodel and the nutrient submodel. The runoff submodel 477
is the driver of erosion and nutrient dynamics. Each of these three submodels are 478
briefly outlined here, and full details are in Wainwright and Parsons (2002), Parsons 479
et al. (1997), Wainwright et al. (2008a, b, c), Mueller et al. (2007) and Turnbull 480
et al. (2010). 481

The hydrological component of MAHLERAN uses a simple infiltration model 482
to generate infiltration- and saturation-excess runoff (Wainwright and Parsons 483
2002). The infiltration rate is simulated using the Smith-Parlange approach (Smith 484
and Parlange 1978). Runoff is routed over the hillslope using a kinematic wave 485
approximation of the St Venant equations (Wainwright and Parsons 2002), with flow 486
routing in the direction of steepest descent from cell to cell (in cardinal directions) 487
over a finite-difference grid (Scoging et al. 1992), using a finite-difference solution 488
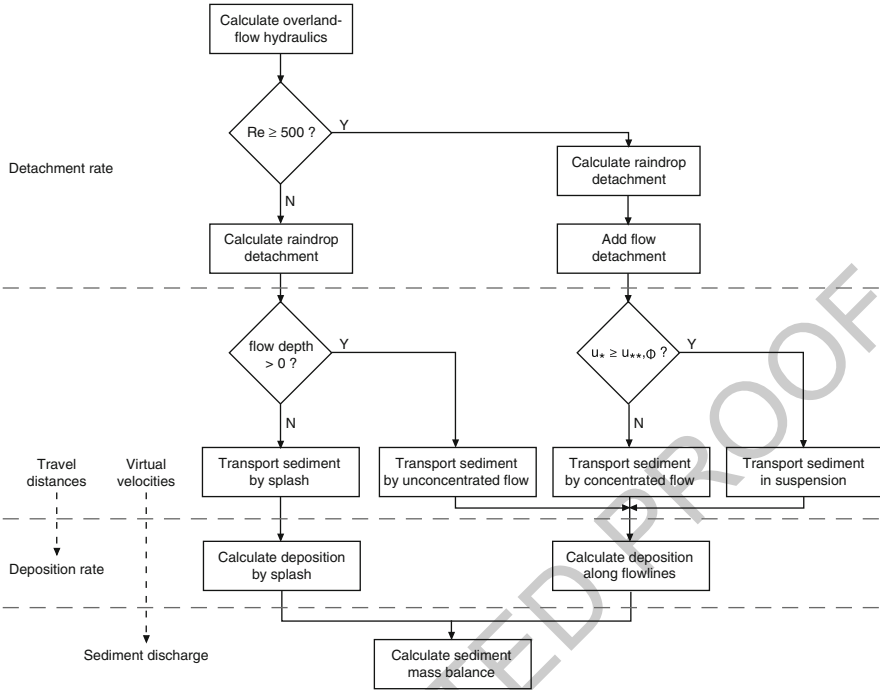
Fig. 7.12 Structure of the erosion submodel of MAHLERAN. Summary of the algorithms used in the erosion submodel of MAHLERAN. The main components in terms of detachment and the use of travel distance and virtual velocity to estimate sediment discharge are highlighted (Source: Wainwright et al. 2008a)

(Euler backward difference form; Scoging et al. 1992). Flow velocity is determined 489
dynamically using the Darcy-Weisbach flow equation. 490

To achieve better prediction of soil erosion by runoff, process-based models are 491
required (Parsons et al. 1997). The erosion submodel of MAHLERAN (Fig. 7.12), 492
and considers the interaction of both raindrop detachment, splash, unconcentrated 493
and concentrated erosion as bedload and in suspension, which is necessary since the 494
relative balance of these processes is the most critical control on the resulting pattern 495
of erosion (Wainwright et al. 2008a). The erosion submodel is based on the concept 496
of entrainment and travel distances of sediment in six particle size classes: $<63\,\mu$m, 497
$63\,\mu$m –0.25 mm, 0.5–2 mm, 2–12 mm and >12 mm. Further details can be found 498
in (Wainwright et al. 2008a). Sediment detachment and transport is simulated for 499
four conditions (Wainwright et al. 2008a): 500

- erosion as a function of raindrop detachment and transport occurs by splash when 501
  no flow is present; 502
- unconcentrated overland flow erosion simulated using raindrop detachment rates 503
  that are modified to account for the protective effects of the surface-water layer; 504

- transport by mixed unconcentrated and concentrated flow ($500 \leq Re < 2,000$) (*Re* 505 is the flow Reynolds number); 506
- transport by concentrated flow ($Re > 2,000$). 507
- Sediment deposition is modelled using a transport-distance approach, whereby 508 the distribution function of travel distances of particles transported via the dif- 509 ferent mechanisms and flow conditions enables determination of the deposition 510 rates at each point along the transport pathway. 511

Dissolved nutrients are modelled conservatively according to an advection- 512 dispersion model (Havis et al. 1992; Walton et al. 2000b), in which the mass transfer 513 of nutrients from the soil surface to runoff is driven by: (i) diffusion of dissolved 514 nutrients from the soil interstices by movement of soil water into the overland 515 flow; (ii) desorption of the nutrients from soil particles into the overland flow; 516 (iii) dissolution of solid phase nutrients into the soil water or overland flow, and 517 (iv) scouring of solid phase nutrients by hydraulic forces and subsequent transport 518 and moving dissolution. A mass-transfer coefficient is used to lump together the 519 mechanisms of mass transfer (Wallach and van Genuchten 1990; see Muller et al. 520 2007b for more detail). Particle-bound nutrients are modelled as a function of 521 the nutrient concentration associated with each particle-size class and the amount 522 of sediment transported within each particle size class. Particle-bound nutrient 523 dynamics are modelled conservatively since it is assumed that there is no adsorption 524 or desorption of particle-bound nutrients during transport (Viney et al. 2000). 525

MAHLERAN has been extensively evaluated for different conditions over dryland 526 hillslopes with different types of vegetation, for different antecedent soil-moisture 527 conditions and for rainfall events of varied magnitudes. Testing of the runoff 528 submodel of MAHLERAN for a range of rainfall events over grassland and shrubland 529 at the Sevilleta National Wildlife Refuge in central New Mexico shows that the 530 runoff model generally performs well, although over shrubland there are some 531 discrepancies with the timing of modelled peak discharge (Fig. 7.13). An extensive 532 evaluation of the erosion component of MAHLERAN for sites at the Walnut 533 Gulch Experimental watershed in southern Arizona demonstrates that MAHLERAN 534 performs well when simulating the total amount of sediment eroded during a runoff 535 event (Wainwright et al. 2008b, c). However, uncertainties introduced by the limited 536 amount of data available for parameterising detachment characteristics as a function 537 of soil-particle size, mean that the proportion of fine sediment relative to coarse 538 sediment is over-estimated by the model. In order to improve further the process- 539 based understanding of erosion processes in drylands, continued laboratory-based 540 experimentation is being undertaken to improve the ability to parameterize such 541 models. Testing of the dissolved nutrient component of MAHLERAN indicates 542 that the conservative modelling of event-based nutrient dynamics is inadequate 543 because intra-event nutrient dynamics do not behave conservatively (Turnbull et al. 544 2011), and that parameterizing initial soil-nutrient content in event-based models is 545 challenging because biogeochemical cycling in drylands is so temporally variable 546 (Hartley and Schlesinger 2000; McCally and Sparks 2009). However, the approach 547 employed to simulate particle-bound nutrients yields satisfactory results, with 548
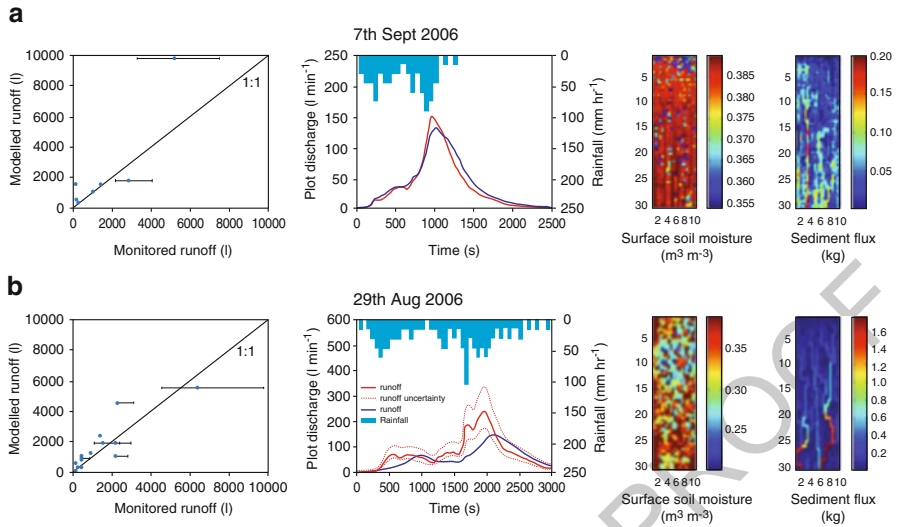
Fig. 7.13 Examples of testing the runoff submodel for (**a**) grassland and (**b**) shrubland. The plots on the *left* compare total event monitored runoff with total event modelled runoff, the plots in the *centre* show the monitored and modelled hydrographs for a single event, and the plots on the *right* show example outputs of spatial maps of water and soil resource redistribution during runoff events over 10 × 30 m grassland and shrubland plots at the Sevilleta National Wildlife Refuge, NM

excellent results for smaller runoff events, and an underestimation of modelled particle-bound nutrient yields for the largest events monitored (Turnbull et al. 2010).

Mueller et al. (2007) applied MAHLERAN to investigate the redistribution of water and soil resources over different types of vegetation boundaries (grassland, creosotebush, tarbush and mesquite; all of which differ in terms of their spatial characteristics, microtopography and influence on soil properties) in the Jornada Basin, New Mexico (32°31′N, 106°47′W; Fig. 7.14).

In this application, MAHLERAN was run with a model cell size of 10 × 10 m and a time resolution of 1 s (Mueller et al. 2007). They evaluated fluxes of water, soil and plant-essential nutrients t 20-m intervals along 60-m wide transects through the vegetation boundaries, extending 140 m upslope of the boundary and 140 m downslope of the boundary (Fig. 7.15). Total fluxes at each point along transects were calculated as the sum of fluxes at that interval (across the 60-m width), scaled by dividing the length of strips to determine an effective average flux in m^3 flux per metre vegetation boundary (i.e. a unit flux across the boundary). Results of this study (Fig. 7.16) are presented as percentage relative changes in fluxes across the vegetation boundaries, since this metric enables the direct comparison of fluxes across different vegetation boundaries.

To investigate how the redistribution of water and soil resources changes over the vegetation boundaries, a 5-min duration rainfall event with rainfall intensity of 109.7 mm h^{-1} (a storm with a 10-year return interval at the site (Wainwright 2005))

AQ7
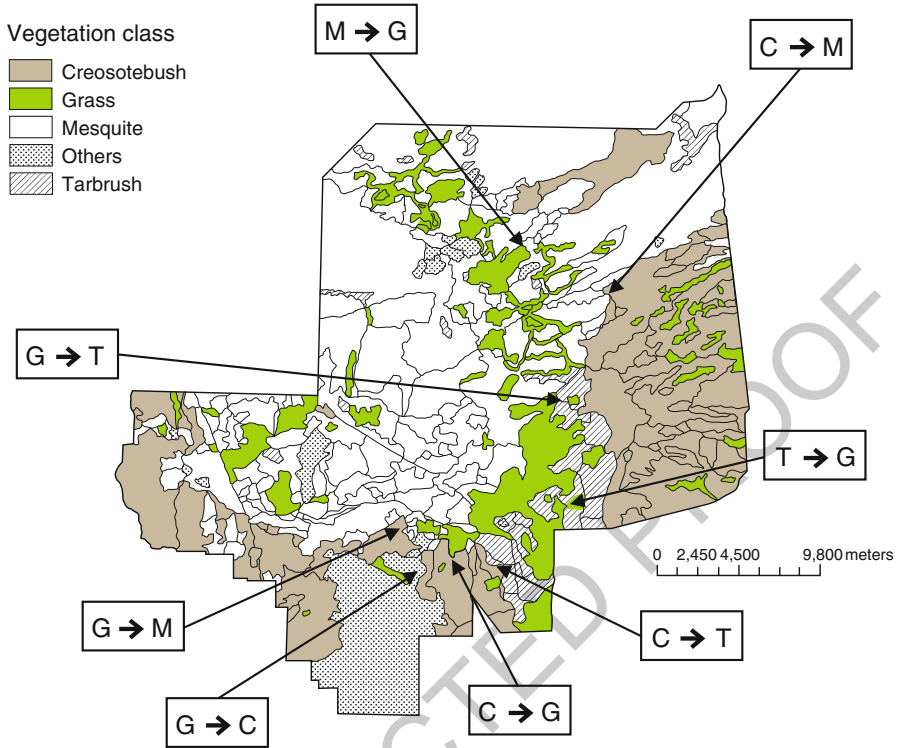
Fig. 7.14 Map showing the locations of vegetation-boundary scenarios within the Jornada Basin (map data provided by the Jornada Exprimental Range Agricultural Research Service, US Department of Agriculture, Las Cruces, New Mexico). *G* is grassland, *M* is mesquite shrubland, *C* is creosotebush shrubland and *T* is tarbush shrubland (Reprinted from Mueller et al. (2007), 91–100, Copyright (2007), with permission from Elsevier)

was simulated for each of the vegetation boundaries. Simulation results show that at vegetation boundaries where shrubs are upslope of grasses, there is a substantial decrease in water flux once the boundary is crossed (Fig. 7.16), with most pronounced decreases for transitions from mesquite to grassland and from tarbush to grassland across the vegetation boundaries. Therefore, grasses that are downslope of shrublands are able to effectively capture and utilize water that is lost from upslope shrublands. These results are directly linked to those obtained from Ecohyd-HydroVeg simulations (Sect. 7.4), whereby more vegetation cover leads to less runoff, thus representing a critical feedback between runoff and erosion dynamics with vegetation growth. Changes in sediment flux over the vegetation boundaries show more complex behaviour, whereby for the shrubland to grassland vegetation boundaries, sediment flux is relatively constant over the shrubland, and increases for a short distance once the vegetation boundary is crossed because of a rise in the detachment rate because of an abrupt change in particle-size distribution
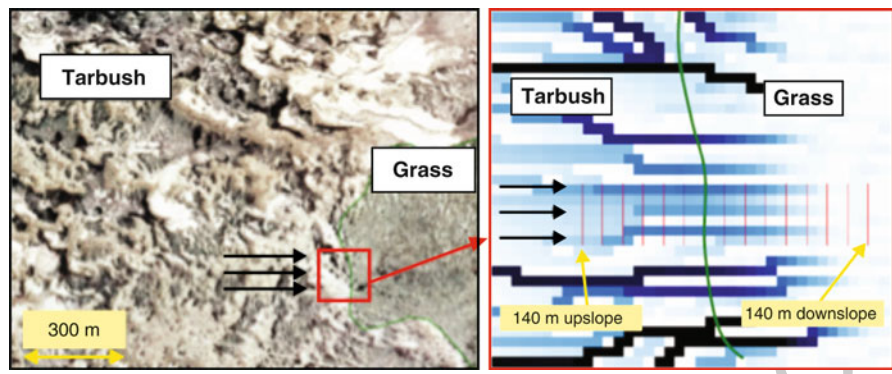
Fig. 7.15 Example of a Tarbush-Grass vegetation boundary over which water and soil resource redistribution was modelled (*left*). *Arrows* show the predominant flow direction. Close-up of the vegetation boundary (*right*) which is marked by the solid *gray line*, showing the total water flux over the boundary (modelled using MAHLERAN, and the area over which fluxes are modelled – extending from 140 m upslope of the vegetation boundary to 140 m downslope of the boundary. *Vertical lines* show the points along the transect over which fluxes were investigated (Reprinted from Mueller et al. 2007, 91–100, Copyright (2007), with permission from Elsevier)

AQ8

(Mueller et al. 2007). Following this initial increase once the vegetation boundary is crossed, sediment flux rates declines, with grasslands retaining sediments eroded from upslope. For the grassland to shrubland vegetation boundaries, sediment flux is greatly elevated in the shrubland. The behaviour of nutrient fluxes across the vegetation boundaries is the opposite of water fluxes, with results showing an increase in nutrient fluxes moving downslope from shrubland to grassland (Mueller et al. 2007).

These modelling results suggest that the redistribution of water and nutrients during rainfall events could have great implications for the stability of vegetation boundaries. For example, a shrub to grass vegetation boundary may be stable when nutrient losses in runoff from grassland are in balance with nutrient replenishment rates by nutrient cycling in grasslands, along with the replenishment of nutrients in runoff from upslope shrublands (Mueller et al. 2007). However, a vegetation boundary may become unstable if grasses lose their ability to sequester and retain nutrients. For example, overgrazing may decrease soil infiltration rate due to soil compaction and increase the connectivity of bare areas, rendering the grassland more "leaky" with reduced ability to capture and retain resources from upslope shrubland, potentially leading to instability. These modelling results suggest that the development of islands of fertility are only one form of small-scale change associated with degradation, and that changes in connectivity are important. Thus, research efforts need to continue to focus on changes in connectivity across landscape scales, since these changes in connectivity and ecogeomorphic feedbacks associated with them are important potential driving mechanisms for catastrophic changes in these systems (Turnbull et al. 2008, 2012).
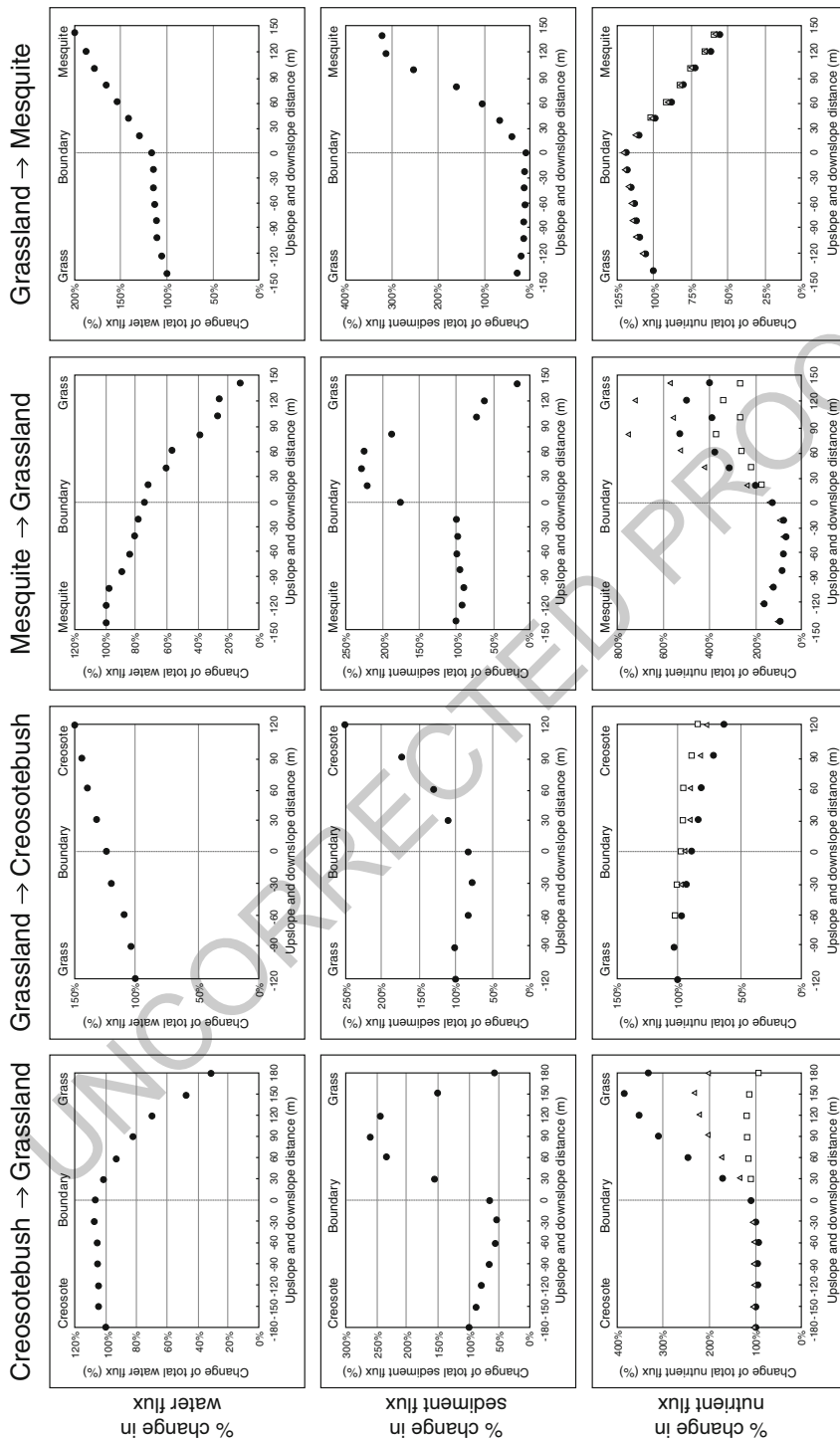
Fig. 7.16 Simulated water, sediment and nutrient fluxes across vegetation boundaries. In the *bottom row* of plots, Δ = ammonium, $\blacksquare$ = Nitrate, $\square$ = Phosphorus (Reprinted from Mueller et al. 2007, 91–100, Copyright (2007), with permission from Elsevier)

7.7 Modelling the (Co-)evolution of Vegetated Aeolian Landscapes

Vegetation cover and its spatial distribution not only affect surface runoff and hydrologically mediated sediment transport, but also they affect aeolian processes. Aeolian processes play an important role in arid and semi-arid regions (discussed in Sect. 5.6). Nearly 20 % of drylands in marginal agriculture regions are underlain by aeolian sand deposits that are currently kept mostly dormant by various degrees of vegetation coverage (Thomas 1999), and it is feared that these dormant dune fields in semi-arid regions may become reactivated (Thomas et al. 2005), leading to increased soil erosion as well as dust emissions. Furthermore, regional degradation and conversion of grasslands to deteriorating shrublands is accelerating (Okin et al. 2006; Grover and Musick 1990), allowing for an increased activity in aeolian erosion, sediment transport and deposition on developing bare surfaces. This increase in aeolian erosion, sediment transport and deposition is often associated with self-organized redistribution of nutrients and sediments leading to a catastrophic shift in the ecosystem state (Scheffer et al. 2001), and the development of a spatial pattern of 'islands of fertility' in the form of nebkha dune fields (Barbier et al. 2006; Tengberg 1995; Wang et al. 2006). This self-organized co-evolution of shrub plant and dune landform results from positive feedbacks between plant growth and local sediment deposition – in the context of plant physiology, sediment controls, and climate.

The impact of vegetation on aeolian sand transport is primarily understood through its effects on near-surface airflow. The enhanced surface roughness of vegetated surfaces decreases the shear stress on the bed and increases the shear-velocity threshold required for sand transport as vegetation elements partially absorb the force of the wind (Lettau 1969). Furthermore, the surface area available for transport is physically reduced. These effects have been investigated on the scale of individual vegetation elements – shrubs and grass clumps (Gillies et al. 2000) – and over surfaces covered with varying degrees of vegetation density (Wolfe and Nickling 1993). Individual shrubs and/or clusters of surface plants act as sediment traps, inducing local deposition on an otherwise potentially deflating surface, and leading to the initiation and growth of shadow dunes (Hesp 1981). In dryland environments there is a great variety of plant species that induce nebkha development, including substantial woody shrubs, like *Artemisia* (sagebrush), *Prosopis* (mesquite) and *Tamarix* (salt cedar), as well as fast-growing ground-hugging plants like *Arctotheca*, *Gazania*, *Zygophyllum*, *Ziziphus*, and *Acacia* (Fig. 7.17). Dense and vertically growing plant species, particularly the woody shrubs, pose a significant obstacle to the wind and consequently form high and relatively steep sided nebkhas, while the ground-hugging plant species more often produce lower and more extended dome-shaped mounds (Hesp and McLachlan 2000). Nebkha shapes may be semi-circular or with an aerodynamic tail of sediment deposit if located in a unidirectional wind regime.

While it is possible to simulate the three-dimensional airflow dynamics and associated sediment transport and deposition processes on and around an individual

Fig. 7.17 Nebkhas on a deflation plane near Akhfenir, Southwest Morocco. Sand transport is predominantly from *left* toward the *right* (sand trapped inside and downwind of the plant clusters)

nebkha dune – using CFD applications for example – CA models are a potent 651
alternative for simulating the complex and self-organizing feedback processes of 652
initiation and evolution of nebkhas at a dunefield scale. The strength of such 653
models is their capacity to identify and explore the key processes that underlie the 654
complexity without involving the excessive number of coefficients, parameters, and 655
assumptions of many detailed reductionist models. 656

The DECAL model (Baas and Nield 2007) is based on a CA algorithm for 657
dune evolution developed by Werner (1995) that was adapted and extended to 658
incorporate the effects of and feedbacks on vegetation in the aeolian environment 659
(Baas 2002). The 3D model space consists of a grid over which discrete 'slabs' 660
of sand are transported along a 'wind' direction between neighbouring cells. The 661
self-organizing aggregation and migration of heaps of slabs is only limited by 662
avalanching to maintain a maximum angle of repose and a 'shadow-zone' behind 663
piles to mimic the forced deposition and no-erosion in the downwind wake of 664
topography. The erosion and deposition of slabs is governed by local probabilities 665
that are determined from the degree of vegetation cover on each cell, while the 666
impact of the net sedimentation balance on the plants in turn is mimicked by 667
annual growth and decline functions that increase or decrease the local vegetation 668
coverage. The algorithm has been expanded to include the effects of multiple types 669
of vegetation and it has proved highly successful in replicating realistic-looking 670
parabolic dunes with trailing ridges and deflation planes as well as nebkha dunes 671
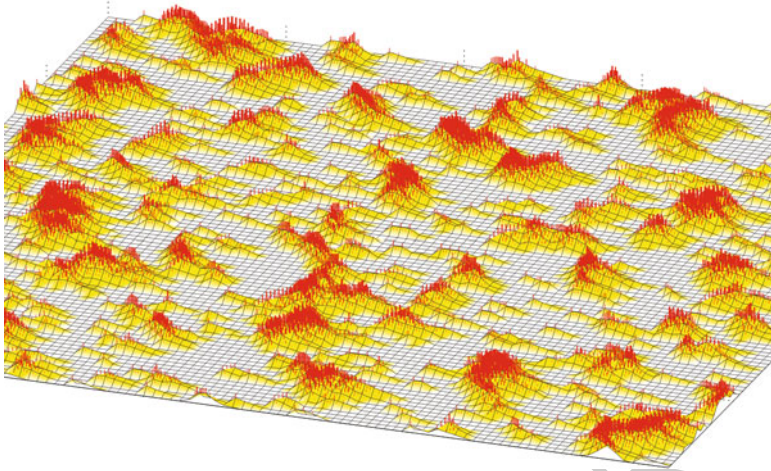
Fig. 7.18 DECAL simulation of nebkha dune field evolved from an initially flat surface under the influence of a mesquite-type shrub vegetation, showing classic aerodynamic tails. Density and size of *red* sticks indicate levels of shrub effectiveness. Sediment transport direction from *upper-left* to *lower-right* of view. Grid resolution is 1.0 m

with lee-side deposition tails (Fig. 7.18), under the influence of vegetation elements that mimic plant species such as marram grass and creeping willow in a costal environment, and mesquite or tamarisk shrubs in a semi-arid environment (Nield and Baas 2008a).

The DECAL model has been used to explore the potential evolution of dune landscapes in response to changes in sediment transport conditions and vegetation vitality (e.g. through climate change) as well as external perturbations, such as wildfires and anthropogenic effects (Nield and Baas 2008b). Simulations of the overall change in vegetation cover as the landscape develops from a flat, barren surface, agree well with field observations of continental semi-arid dune fields in the Great Plains, Canada, as observed by Wolfe et al. (2000). Simulations over longer time scales show evolutionary sequences with thresholds, relaxation periods, and equilibration, and the model has revealed how the amplitude, frequency, and timing (relative to the evolutionary stage) of various perturbations has wildly differential effects on the resultant landscape response. Simulations of dryland environments with mesquite- or sagebrush-type vegetation, meanwhile, demonstrate the important control of initial sediment availability and supply on the subsequent size, shape and spatial distribution of nebkhas, and have also yielded more fundamental insights into the relationship between abiotic sediment transport processes and biotic components in an ecogeomorphic system. The model reveals how the vegetation and its interactions appear to impress a characteristic scale on the dynamic system so that size and shape of vegetated dunes are fundamentally controlled by the ecological attributes of the plant species in the environment. Whereas bare sand dunes are found over several orders of magnitudes in size, dunes developing

under the influence of vegetation may thus exhibit a clear restriction in size-   696
range and shape that is fundamentally related to the biological limits of their   697
physiological and photosynthetic potential (Baas 2007). The model is now being   698
used to investigate rigorously the precise biotic controls on dune field development   699
in a quantitative framework, by linking vegetation parameters to potential system   700
attractors and typical evolutionary trajectories determined from topographic and   701
ecological metrics (Baas and Nield 2010).   702

7.8 Towards a Fully Integrated Model Framework   703
to Simulate Feedbacks Between Biotic and Abiotic   704
Ecosystem Structure and Function: Problems   705
and Challenges   706

Having discussed sets of ecological and geomorphic processes individually in the   707
preceding sections, we now return to the issue of linking ecological processes and   708
geomorphic processes together more holistically. As suggested in Sects. 7.2 and   709
7.3 we can explore the development of patterns using deterministic and stochastic   710
models of pattern formation; however, fully integrated ecogeomorphic models are   711
required to explore the *processes* of pattern formation which is critical to understand   712
land degradation in drylands. The models outlined in this chapter demonstrate that a   713
variety of modelling tools are available to simulate pattern formation in drylands   714
both deterministically and stochastically, and to simulate processes that lead to   715
pattern formation in drylands. A practical limitation of the modelling approaches   716
explored in this chapter, is that they are limited in their spatial and/or temporal ex-   717
tent – largely due to access to suitable computational resources, or the willingness of   718
researchers to use them. However, the main limitation to developing fully integrated   719
ecogeomorphic models is largely conceptual. Although great leaps have been made   720
over recent years in understanding some of the linkages between ecological and   721
geomorphic processes (discussed in Chaps. 4 and 5), there still remain fundamental   722
gaps in our understanding of their interactions at different spatial and temporal   723
scales. A critical challenge in conceptualizing the ecogeomorphic system rests in   724
reconciling the level of process representation that is needed to simulate multi- and   725
cross-scale feedbacks between ecological and geomorphic processes.   726

In terms of vegetation dynamics for example, plant-recovery time following a   727
disturbance will be in-part determined by plant phenology and rainfall seasonality.   728
However, because of the annual time step in ECOTONE, such effects cannot be rep-   729
resented. Furthermore, not all disturbances impact all plants uniformly; for example,   730
mesquite shrubs are commonly avoided both by foot, vehicle traffic, and grazers   731
which may to an extent explain their dominance in disturbed areas, whereas grasses   732
indigenous to the same environment are often disturbed by trampling and over-   733
grazing. Therefore, the extent to which species-specific responses are represented   734
in vegetation models could have a great effect on simulated vegetation dynamics.   735

In terms of hydrological and geomorphic processes, MAHLERAN is an event-based 736
model that simulates runoff, erosion and nutrient dynamics during rainfall events, 737
meaning that antecedent conditions such as soil-moisture content, soil-nutrient 738
content and vegetation cover have to parameterized for each model run. The detailed 739
datasets available for parameterizing antecedent conditions are rarely available, 740
which thus highlights a great limitation event-based modelling approaches. 741

The extensive expertise required to develop, parameterize and test the process- 742
specific models explored in this chapter highlight the extent to which developing 743
ecogeomorphic modelling tools is a major challenge, for both conceptual and 744
technical reasons. A key issue facing the development of ecogeomorphic models, 745
is whether or not the focus should be on making the most of existing resources by 746
coupling existing models (legacy models) that each simulate an isolated components 747
of the system, or if the focus should be on developing new integrated ecogeomorphic 748
models that do not suffer from the constraints (conceptual and technical) imposed 749
by utilizing existing models. There are many different ways in which models can be 750
coupled, ranging from loose coupling to tight coupling (Brandmeyer and Karimi 751
2000). The different approaches to coupling models will have implications for 752
simulating feedbacks across multiple spatial and temporal scales, and simulating 753
emergent phenomena. Thus, the method used to develop an ecogeomorphic model 754
needs to consider its desired purpose. 755

Loosely coupled models share a common interface, which controls data transfer 756
between the coupled models. Advantages of loosely coupling models include: (i) 757
it is a relatively inexpensive way of coupling models; (ii) models need not be 758
written in the same code; (iii) individual models may be continually developed 759
without hindering the interoperability of the coupled model; and (iv) models can 760
be linked with few changes made to the existing code. Disadvantages of loosely 761
coupled modelling approaches include: (i) data-conversion programs or subroutines 762
may be required to insure data interoperability between models (for example, the 763
spatial or temporal aggregation or disaggregation of data); and (ii) maintenance 764
to the interface may be required when the data structure of a model is updated. 765
In tightly coupled models, one model may be embedded inside another, or two or 766
more (sub-) models may run in parallel. Advantages of tightly coupled modelling 767
approaches include: (i) increased flexibility for dynamic feedbacks between model 768
components to occur; (ii) reduced data redundancy; (iii) potential for common 769
data storage. Disadvantages of tightly coupled approaches include: (i) the necessity 770
for source-code modification; (ii) detailed understanding of each model; and (iii) 771
ensuring compatibility between all common elements. Model coupling may also 772
extend beyond tight coupling, to form a new "integrated model", in which all model 773
components are dynamically linked, model components have common data storage, 774
and a single model language is used. The development of integrated models is 775
probably the most costly form of modelling, since it usually necessitates coding 776
from scratch, and requires a high level of expert knowledge of all processes 777
represented within the model – hence the need for inter-/multi-disciplinarity to 778
ensure the success of integrated models. The extent to which models need to be 779
coupled is in part dependent on the speed and frequency of feedbacks between 780

different processes that occur in the system to be modelled. If feedbacks occur 781
relatively slowly, then loose coupling may suffice. However, if feedbacks occur 782
relatively quickly, then tight coupling or integrated models are necessary. 783

The starting point for tightly coupled or integrated ecogeomorphic modelling 784
must be the conceptualization of the system in question, whereby key processes and 785
the spatial and temporal scales over which they operate are identified. A critical 786
component of this conceptualization process is determining the elements that will 787
link each model (for example, soil moisture, soil texture, soil-nutrient content, plant 788
biomass). These common elements have to be compatible, for example, the ways 789
in which water and plant biomass are represented. Furthermore, the representation 790
of a process needs to be consistent between models that are being coupled – 791
for example, two models might use different process descriptions to resolve soil- 792
moisture dynamics, which might thus lead to conflicting outcomes for the same 793
process (Janssen et al. 2011). If models are to be meaningfully coupled or integrated, 794
it is essential that differences in their spatial and temporal extents and scales are 795
reconciled (Brandmeyer and Karimi 2000). Aggregation/disaggregation techniques 796
may need to be used to reconcile differences in spatial and temporal scales, but doing 797
so requires in-depth knowledge of how system properties and processes scale. The 798
spatial and temporal domains of an ecogeomorphic model will depend largely on the 799
purpose of modelling. Therefore, when conceptualizing the system, the spatial and 800
temporal domains of the modelling study must be carefully considered. For instance, 801
the important ecogeomorphic processes and their critical spatial and temporal scales 802
when studying hillslope-scale processes at the timescale of rainfall-runoff events 803
may be greatly different to those when studying the evolution of deserts over multi- 804
decadal timescales. The coupling of two or more models could result in exceedingly 805
high parameterization requirements, which may potentially limit the ease with 806
which such models may be used in a meaningful way. Care therefore needs to 807
be taken to ensure that parameterization requirements for each model component 808
remain as low as possible. As multiple models are coupled, and as parameterization 809
requirements increase, there is great potential for the propagation of uncertainty. 810
Uncertainty is, to some extent, inherent in all modelling approaches, and is derived 811
from multiple sources, such as uncertainty in process understanding, process 812
representation and model parameterization. As models become more complicated – 813
as is the case with coupled models – more uncertainty is introduced (Ascough 814
et al. 2008), and the compound effects of multiple sources of uncertainty can be 815
great (see also the discussion in Chap. 10). Identifying sources of uncertainty, and 816
recognizing and quantifying its consequences within modelling-based studies, is 817
a major challenge that needs to be addressed. A more detailed consideration of 818
uncertainty is provided in Chap. 10. 819

Land degradation continues to occur at alarming rates in drylands, and our 820
existing approaches to understand the effects of environmental drivers and human- 821
induced disturbances on ecogeomorphic processes in drylands are inadequate. In 822
order to simulate these processes in drylands, approaches used to develop ecogeo- 823
morphic models need to be as simple as possible, but no simpler, in order to expedite 824
the process of model development, model parameterization, model testing, and be 825

used with ease by a wide community. The abundance of models that have been de- 826
veloped over recent decades to simulate isolated components of the ecogeomorphic 827
system represent an ideal starting point from which to develop coupled or integrated 828
ecogeomorphic models. There are likely to be many advantages of pursuing tightly 829
coupled approaches to ecogeomorphic modelling as opposed to loosely coupled 830
or integrated approaches. Using tightly coupled modelling approaches enable 831
feedbacks to be represented at appropriate spatial and temporal scales. Component 832
models can be updated to reflect ongoing advances that are made in process 833
understanding in individual disciplines (although maintenance and model testing 834
will be required to ensure ongoing compatibility of models when components are 835
updated). Because tightly coupled modelling approaches make use of available 836
resources, their development may be much more rapid and more cost-effective than 837
integrated models. A strong argument for tightly coupled modelling is that it enables 838
evaluation of what goes wrong when it is applied outside the "comfort zone" of 839
one's own discipline, or away from initial conceptualizations of space and time. 840

Ultimately, if patterns and processes are important in understanding land degra- 841
dation in drylands, we can only gain limited understanding by using detailed models 842
that do not, or cannot represent pattern, or by looking at models that look at patterns, 843
but not the processes in operation. In developing ecogeomorphic models, either 844
by coupling or integrating models, these different perspectives need to be brought 845
together. Critically, the ecogeomorphic modelling and field experimentation need to 846
be carried out in tandem, with field experimentation informing the conceptualization 847
and development of ecogeomorphic models, and ecogeomorphic models servicing 848
as a tool to benefit the design of a new generation of ecogeomorphic field 849
experiments to help resolve the remaining unknowns of pattern-process linkages 850
in drylands. 851

References 862

AQ9

Ascough JC, Maier HR, Ravalico JK, Strudley MW (2008) Future research challenges for 863
incorporation of uncertainty in environmental and ecological decision-making. Ecol Model 864
219:383–399 865
Atlas of Namibia Project (2002) Directorate of Environmental Affairs, Ministry of Envi- 866
ronment and Tourism. http://uni-koeln.de/sfb389/e/e1/download/atlas_namibia/pics/climate/ 867
rainfall-annual.jpg. Accessed Oct 2011 868

Baas ACW (2002) Chaos, fractals and self-organization in coastal geomorphology: simulating dune landscapes in vegetated environments. Geomorphology 48:309–328. doi:10.1016/S0169-555X(02)00187-3

Baas ACW (2007) Complex systems in aeolian geomorphology. Geomorphology 91:311–331. doi:10.1016/j.geomorph.2007.04.012

Baas ACW, Nield JM (2007) Modelling vegetated dune landscapes. Geophys Res Lett 34:L06405. doi:10.1029/2006GL029152

Baas ACW, Nield JM (2010) Quantifying the evolution of vegetated aeolian landscapes: ecogeomorphic state variables and phase-space construction. Earth Surf Process Landf 35:717–731. doi:10.1002/esp.1990

Barbier N, Couteron P, Lejoly J, Deblauwe V, Lejeune O (2006) Self-organized vegetation patterning as a fingerprint of climate and human impact on semi-arid ecosystems. J Ecol 94:537–547

Bartley R, Roth CH, Ludwig J, McJannet D, Liedloff A, Corfield J, Hawdon A, Abbott B (2006) Runoff and erosion from Australia's tropical semi-arid rangelands: influence of ground cover for differing space and time scales. Hydrol Process 20:3317–3333

Brandmeyer JE, Karimi HA (2000) Coupling methodologies for environmental models. Environ Model Softw 15:479–488

Bugmann H (2001) A review of forest gap models. Clim Change 51:259–305

Cammeraat LH (2004) Scale dependent thresholds in hydrological and erosion response of a semi-arid catchment in Southeast Spain. Agric Ecosyst Environ 104:317–332

Coffin DP, Urban DL (1993) Implications of natural-history traits to system-level dynamics – comparisons of a grassland and a forest. Ecol Model 67:147–178

Couteron P, Lejeune O (2001) Periodic spotted patterns in semi-arid vegetation explained by a propagation-inhibition model. J Ecol 89:616

Cross MC, Hohenberg PC (1993) Pattern-formation outside of equilibrium. Rev Mod Phys 65:851

Devitt DA, Smith SD (2002) Root channel macropores enhance downward movement of water in a Mojave Desert ecosystem. J Arid Environ 50:99–108

Easterling DR, Meehl GA, Parmesan C Changon SA, Karl TR, Mearns LO (2000) Climate extremes: observations, modelling and impacts. Science 289:2068–2074

Eppinga M, Rietkerk M, Borren W, Lapshina E, Bleuten W, Wassen M (2008) Regular surface patterning of peatlands: confronting theory with filed data. Ecosystems 11:520–538

Esteban J, Fairen V (2006) Self-organized formation of banded vegetation patterns in semi-arid regions: a model. Ecol Complex 3:109–118

Fischlin A et al (2007) Ecosystems, their properties, goods, and services. In: Parry ML, Canziani OF, Palutikof JP (eds) Climate change 2007: impacts, adaptation and vulnerability. Contribution of Working Group II to the fourth assessment report of the Intergovernmental Panel on Climate Change. Cambridge University Press, Cambridge

Gleason K, Krantz WB, Caine N, George JH, Gunn RD (1986) Geometrical aspects of sorted patterned ground in recurrently frozen soil. Science 232:216–220

Goslee SC, Peters DCP, Beck KG (2001) Modeling invasive weeds in grasslands: the role of allelopathy in Acroptilon repens invasion. Ecol Model 139:31–45

Goslee SC, Peters DCP, Beck KG (2006) Spatial prediction of invasion success across heterogeneous landscapes using an individual-based model. Biol Invasion 8:193–200

Green RE, Ampt GA (1911) Studies on soil physics: 1. Flow of air and water through soils. J Agric Sci 4:1–24

Grover HD, Musick HB (1990) Shrubland encroachment in Southern New Mexico, USA – an analysis of desertification processes in the American Southwest. Clim Change 17:305–330

Grubb PJ (1977) The maintenance of species-richness in plant communities: the importance of the regeneration niche. Biol Rev 52:107–145

Hargreaves GH (1974) Estimation of potential and crop evapotranspiration. Trans ASAE 17:701–704

Hartley AE, Schlesinger WH (2000) Environmental controls on nitric oxide emission from northern Chihuahuan desert soils. Biogeochemisrty 50:279–300

AQ10

Havis RN, Smith RE, Adrian DD (1992) Partitioning solute transport between infiltration and overland flow under rainfall. Water Resour Res 28:2569–2580

Hesp PA (1981) The formation of shadow dunes. J Sed Petrol 51:101–112

Hesp P, McLachlan A (2000) Morphology, dynamics, ecology and fauna of Arctotheca populifolia and Gazania rigens nabkha dunes. J Arid Environ 44:155–172

HilleRisLambers R, Rietkerk M, Van den Bosch F, Prins HHT, de Kroon H (2001) Vegetation pattern formation in semi-arid grazing systems. Ecology 82:50–61

Hochstrasser T (2001) Pattern and process at a desert grassland-shrubland ecotone. Colorado State University, Fort Collins

Hochstrasser T and Peters DPC (2005) Ecotone manual. Technical report ERDC/CERL CR-05-2. US Army Engineer Research and Development Center, Construction Engineering Research Laboratory, Champaign

Hochstrasser T, Peters DPC and Fehmi JS (2005) Simulation of vegetation recovery from military disturbances on Fort Bliss. Technical Report ERDC/CERL TR-05-39. US Army Engineer Research and Development Center, Construction Engineering Research Laboratory, Champaign

Huxman TE, Wilcox BP, Breshears DD, Scott RL, Snyder KA, Small EE, Hultine K, Pockman WT, Jackson RB (2005) Ecohydrological implications of woody plant encroachment. Ecology 86:308–319

Jeltsch F, Milton SJ, Dean WRJ, Van Rooyen N (1996) Spacing and coexistence in semiarid savannas. J Ecol 84:583–595

Jeltsch F, Blaum N, Claasen N, Eschenbach A, Grohmann C, Gröngröft A, Joubert DF, Horn A, Lohmann D, Linsenmair KE, Lück-Vogel M, Medisnski TV, Meyfahrt S, Mills A, Petersen A, Popp A, Poschlod P, Reisch C, Rossmanith E, Rubilar H, Schütze S, Seymour C, Simmons R, Smit GN, Strohbach M, Tews J, Tietjen B, Wesuls D, Wichmann M, Wieczorek M, Zimmermann I (2010a) Impacts of landuse and climate change on the dynamics and biodiversity in the Thornbush Savanna Biome. In: Hoffman MT, Schmiedel U, Jürgens N (eds) Biodiversity in southern Africa, vol 3, Implications for landuse and management. Klaus Hess Publishers, Göttingen/Windhoek, pp 33–74

Jeltsch F, Blaum N, Lohmann D, Meyfahrt S, Rossmanith E, Schütze S, Tews J, Tietjen B, Wichmann M, Wieczorek M (2010b) Modelling vegetation change in arid and semi-arid savannas. In: Schmiedel U, Jürgens N (eds) Biodiversity in southern Africa, vol 2, Patterns and processes at regional scale. Klaus Hess Publishers, Göttingen/Windhoek, pp 274–282

Jeltsch F, Tietjen B, Blaum N, Rossmanith E (2010c) Population and ecosystem modeling of land use and climate change impacts on savanna dynamics. In: Hill MJ, Hanan NP (eds) Ecosystem function in savannas: measurement and modeling at landscape to global scales. CRC Press, Boca Raton, p 623

Kokkonen T, Jolma A, Koivusalo H (2002) Interfacing environmental simulation models and databases using XML. Environ Model Softw 18:463–471

Kuiper SM, Meadows ME (2002) Sustainability of livestock farming in the communal lands of southern Namibia. Land Degrad Dev 13:1–15

Lefever R, Lejeune O (1997) On the origin of the tiger bush. Bull Math Biol 59:263–294

Lefever R, Barbier N, Couteron P, Lejeune O (2009) Deeply gapped vegetation patterns: on crown/root allometry, criticality and desertification. J Theor Biol 261:194

Lettau H (1969) Note on aerodynamic roughness-parameter estimation on the basis of roughness-element description. J Appl Meteorol 8:828–832

Li ZQ, Bogaert J, Nijs I (2005) Gap pattern and colonization opportunities in plant communities: effects of species richness, mortality, and spatial aggregation. Ecography 28:777–790

Loik ME, Breshears DD, Lauenroth WK, Belnap J (2004) A multi-scale perspective of water pulses in dryland ecosystems: climatology and ecohydrology of the western USA. Oecologia 141:269–281

Martinez-Mena M, Albaladejo JA, Castillo VM (1998) Factors influencing surface runoff generation in a Mediterranean semi-arid environment: Chicamo watershed, SE Spain. Hydrol Process 5:741–754

AQ11

McCally CK, Sparks JP (2009) Abiotic gas formation drives nitrogen loss from a desert ecosystem. Science 326:837–840

Ministry of Agriculture, Water and Forestry (2009) Agricultural statistics bulletin (2000–2007). Directorate of Planning, Windhoek

Minnick TJ, Coffin DP (1999) Geographic patterns of simulated establishment of two *Bouteloua* species: implications for distributions of dominants and ecotones. J Veg Sci 10:343–356

Mueller EN, Wainwright J, Parsons AJ (2007) The stability of vegetation boundaries and the propagation of desertification in the American Southwest: a modelling approach. Ecol Model 208:91–101

Nield JM, Baas ACW (2008a) Investigating parabolic and nebkha dune formation using a cellular automaton modelling approach. Earth Surf Process Landf 33:724–740. doi:10.1002/esp.1571

Nield JM, Baas ACW (2008b) The influence of different environmental and climatic conditions on vegetated aeolian dune landscape development and response. Glob Planet Change 64:76–92. doi:10.1016/j.gloplacha.2008.10.002

Norby RJ, Luo YQ (2004) Evaluating ecosystem response to rising CO_2 and global warming in a multi-factor world. New Phytol 162:281–293

Noy-Meir I (1973) Desert ecosystems: environment and producers. Annu Rev Ecol Syst 4:25–51

Okin GS, Gillette DA, Herrick JE (2006) Multi-scale controls on and consequences of aeolian processes in landscape change in arid and semi-arid environments. J Arid Environ 65:253–275

Okin GS, Parsons AJ, Wainwright J, Herrick JE, Bestelmeyer BT, Peters DC, Fredrickson EL (2009) Do changes in connectivity explain desertification. Bioscience 59:237–244

Parker P, Letcher R, Jakeman A, Beck MB, Harris G, Argent RM, Hare M, Pahl-Wostl C, Voinov A, Janssen M, Sullivan P, Scoccimarro M, Friend A, Sonnenshein M, Barker D, Matejicek L, Odulaja D, Deadman P, Lim K, Larocque TP, Fletcher C, Put A, Maxwell T, Charles A, Breeze H, Nakatani N, Mudgal S, Naito W, Osidele O, Eriksson I, Kautsky U, Kautsky E, Naeslund B, Kumblad L, Park R, Maltagliati S, Girardin P, Rizzoli A, Mauriello D, Hoch R, Pelletier D, Reilly J, Olafsdottir R, Bin S (2002) Progress in integrated assessment and modelling. Environ Model Softw 17:209–217

Parsons AJ, Abrahams AD, Luk S (1991) Size characteristics of sediment in interill overland flow on a semi-arid hillslope, Southern Arizona. Earth Surf Process Landf 16:143–152

Parsons AJ, Wainwright J, Abrahams AD, Simanton JR (1997) Distributed dynamic modelling of interrill overland flow. Hydrol Process 11:1833–1859

Parton WJ (1978) Abiotic section of ELM. In: Innis GS (ed) Grassland simulation model. Springer, New York, pp 31–53

Parton WJ, Hartman M, Ojima D, Schimel D (1998) DAYCENT and its land surface submodel: description and testing. Glob Planet Change 19:35–48

Perry GLW, Enright NJ (2006) Spatial modelling of vegetation change in dynamic landscapes: a review of methods and applications. Prog Phys Geogr 30:47–72

Peters DPC (2000) Climatic variation and simulated patterns in seedling establishment of two dominant grasses at a semi-arid-arid grassland ecotone. J Veg Sci 11:493–504

Peters DPC (2002) Plant species dominance at a grassland-shrubland ecotone: an individual- based gap dynamics model of herbaceous and woody species. Ecol Model 152:5–32

Peters DPC, Havstad KM (2006) Nonlinear dynamics in arid and semi-arid systems: interactions among drivers and processes across scales. J Arid Environ 65:196–206

Plackett RL, Burman JP (1946) The design of optimum multifactorial experiments. Biometrika 33:305–325

Rawls W, Brakensiek DL, Saxton KE (1982) Estimation of soil water properties. Trans ASAE 25:1316–1320

Ridolfi L, D'Odorico P, Laio F (2011) Noise-induced phenomena in the environmental sciences. Cambridge University Press, New York

Rietkerk M, Van de Koppel J (1997) Alternate stable states and threshold effects in semi-arid grazing systems. Oikos 79:69–76

Rietkerk M, Dekker SC, De Ruiter PC, Van de Koppel J (2004) Self-organized patchiness and catastrophic shifts in ecosystems. Science 305:1926–1929

Roques KG, O'Connor TG, Watkinson AR (2001) Dynamics of shrub encroachment in an African savanna: relative influences of fire, herbivory, rainfall and density dependence. J Appl Ecol 38:268–280

Sagues F, Sancho JM, García-Ojalvo J (2007) Spatio-temporal order out of noise. Rev Mod Phys 79:829

Sala OE, Lauenroth WK, Parton WJ (1992) Long-term soil water dynamics in the shortgrass steppe. Ecology 73:1175–1181

Scanlon TM, Caylor KK, Levin SA, Rodriguez-Iturbe I (2007) Positive feedbacks promote power-law clustering of Kalahari vegetation. Nature 449:209

Scheffer M, Carpenter S, Foley J, Folke C, Walker B (2001) Catastrophic shifts in ecosystems. Nature 413:591–596

Schwartz M (2006) Numerical modelling of groundwater vulnerability: the example Namibia. Environ Geol 50:237–249

Scoging H, Parsons AJ, Abrahams AD (1992) Application of a dynamic overlandflow hydraulic model to a semi-arid hillslope, Walnut Gulch, Arizona. In: Parsons AJ, Abrahams AD (eds) Overland flow: hydraulics and erosion mechanics. UCL Press, London

Silvertown J, Smith B (1988) Gaps in the canopy – the missing dimension in vegetation dynamics. Vegetation 77:57–60

Smith RE, Parlange JY (1978) A parameter-efficient hydrologic infiltration model. Water Resour Res 14:533–538

Stavi I, Lavee H, Ungar ED, Sarah P (2009) Eco-geomorphic feedbacks in semi-arid rangelands: a review. Pedosphere 19:217–229

Tengberg A (1995) Nebkha dunes as indicators of wind erosion and land degradation in the Sahel zone of Burkina-Faso. J Arid Environ 30:265–282

Thomas DSG (1999) Coastal and continental dune management into the twenty-first century. In: Goudie AS, Livingstone I, Stokes S (eds) Aeolian environments, sediments, and landforms. Wiley, Chichester, pp 105–127

Thomas DSG, Knight M, Wiggs GFS (2005) Remobilization of southern African desert dune systems by twenty-first century global warming. Nature 435:1218–1221

Tietjen B, Zehe E, Jeltsch F (2009) Simulating plant water availability in dry lands under climate change: a generic model of two soil layers. Water Resour Res 45:W01418

Tietjen B, Jeltsch F, Zehe E, Classen N, Groengroeft A, Schiffers K, Oldeland J (2010) Effects of climate change on the coupled dynamics of water and vegetation in drylands. Ecohydrology 3:226–237

Todd RW, Klocke NL, Hergert GW, Parkhurst AM (1991) Evaporation from soil influenced by crop shading, crop residue, and wetting regime. Trans ASABE (Am Soc Agric Biol Eng) 34:0461–0466

Turing AM (1952) The chemical basis of morphogenesis. Philos Trans R Soc Lond Ser B 237:37

Turnbull L, Wainwright J, Brazier RE (2008) A conceptual framework for understanding semi-arid land degradation: ecohydrological interactions across multiple-space and time scales. Ecohydrology 1:23–34

Turnbull L, Wainwright J, Brazier RE (2010) Modelling hydrology, erosion and nutrient transfers over a semi-arid transition from grassland to shrubland in the south-western USA. J Hydrol 388:258–272. doi:10.1016/j.jhydrol.2010.05.005

Turnbull L, Wainwright J, Brazier RE (2011) Nutrient dynamics during runoff events over a transition from grassland to shrubland in south-western USA. Hydrol Process 25:1–17. doi:10.1002/hyp.7806

Turnbull L, Wilcox BP, Belnap J, Ravi S, D'Odorico P, Childers DL, Gwenzi W, Okin GS, Wainwright J, Caylor KK, Sankey T (2012) Understanding the role of ecohydrological feedbacks in ecosystem-state change in drylands. Ecohydrology. doi:10.1002/eco.265

Valentin C, D'Herbes JH, Poesen J (1999) Soil and water components of banded vegetation patterns. Catena 37:1–24

van Palutikof PJ, derGillies JA, Lancaster N, Nickling WG, Crawley DM (2000) Field determination of drag forces and shear stress partitioning effects for a desert shrub (Sarcobatus vermiculatus, greasewood). J Geophys Res 105:24871–24880

Viney NR, Sivapalan M, Deeley D (2000) A conceptual model of nutrient mobilisation and transport applicable at large catchment scales. J Hydrol 240:23–44

Von Hardenberg J, Kletter AY, Yizhaq H, Nathan J, Meron E (2010) Periodic versus scale-free patterns in dryland vegetation. Proc R Soc B 277:1771–1776

Wainwright J (2005) Climate and climatological variations in the Jornada range and neighbouring areas of the US South West. Adv Environ Monit Model 1:39–110

Wainwright J, Bracken LJ (2011) Overland flow and runoff generation. In: Thomas DSG (ed) Arid zone geomorphology, 3rd edn. Wiley, Chichester, pp 235–268

Wainwright J, Parsons AJ (2002) The effect of temporal variations in rainfall on scale dependency in runoff coefficients. Water Resour Res 38: Art. No 1271

Wainwright J, Parsons AJ, Abrahams AD (2000) Plot-scale studies of vegetation, overland flow and erosion interactions: case studies from Arizona and New Mexico. Hydrol Process 14:2921–2943

Wainwright J, Parsons AJ, Müller EN, Brazier RE, Powell DM, Fenti B (2008a) A transport-distance approach to scaling erosion rates: 1. background and model development. Earth Surf Process Landf 33:813–826. doi:10.1002/esp.1624

Wainwright J, Parsons AJ, Müller EN, Brazier RE, Powell DM, Fenti B (2008b) A transport-distance approach to scaling erosion rates: 2 sensitivity and evaluation of Mahleran. Earth Surf Process Landf 33:962–984. doi:10.1002/esp.1623

Wainwright J, Parsons AJ, Müller EN, Brazier RE, Powell DM, Fenti B (2008c) A transport-distance approach to scaling erosion rates: 3. Evaluating scaling characteristics of Mahleran. Earth Surf Process Landf 33:1113–1128. doi:10.1002/esp.1622

Walker BH, Ludwig D, Holling CS, Peterman RM (1981) Stability of semi-arid savanna grazing systems. J Ecol 69:473–498

Wallach R, van Genuchten M (1990) A physically based model for predicting solute transfer from soil solution to rainfall-induced runoff water. Water Resour Res 26:2119–2126

Walton RS, Volker RE, Bristow KL, Smettem KRJ (2000a) Experimental examination of solute transport by surface runoff from low-angle slopes. J Hydrol 233:19–36

Walton RS, Volker RE, Bristow KL, Smettem KRJ (2000b) Solute transport by surface runoff from low-angle slopes: theory and application. Hydrol Process 14:1139–1158

Wang X, Wang T, Dong Z, Liu X, Qian G (2006) Nebkha development and its significance to wind erosion and land degradation in semi-arid northern China. J Arid Environ 65:129–141

Werner BT (1995) Eolian dunes: computer simulation and attractor interpretation. Geology 23:1107–1110

Wolfe SA, Nickling WG (1993) The protective role of sparse vegetation in wind erosion. Prog Phys Geogr 17:50–68

Wolfe SA, Muhs DR, David PP, McGeehin JP (2000) Chronology and geochemistry of late Holocene eolian deposits in the Brandon Sand Hills, Manitoba, Canada. Quat Int 67:61–74

AQ12

AUTHOR QUERIES

AQ1. Please confirm the corresponding author. Also provide department name for Mareike Wieczorek.

AQ2. Please confirm the organization name for John Wainwright.

AQ3. Borgogno et al. (2009), Scarsoglio et al. (2009), Dingman (1994), Joubert et al. (2008), Dodd and Lauenroth (1997), Schwinning and Weiner (1998), Barbour et al. (1977), Hochstrasser et al. (2002), Cole (1995), Yorks et al. (1997), Abrahams and Parsons (1991), Calvo-Cases et al. (2003), Bracken and Croke (2007), Muller et al. (2007a, b), Horton (1945), Gillies et al. (2000), Janssen et al. (2011), Sala et al. (1997) are cited in text but not given in the reference list. Please check.

AQ4. Please provide the appropriate equation number for cross-reference to Eq. 7.7.2.

AQ5. Couteron et al. (2001), Gleason (1986), Wainwright et al. (2005), Brandmeyer et al. (2000) have been changed to Couteron and Lejeune (2001), Gleason et al. (1986), Wainwright (2005), Brandmeyer and Karimi (2000), respectively as per the reference list. Please check if appropriate.

AQ6. Please provide the appropriate figure number for cross-citations to Fig. 7.4.2 and 7.4.3.

AQ7. Please confirm the matching of caption and artwork from Figs. 7.14-7.18. The extra artwork has not be included. Please check.

AQ8. Please provide closing parenthesis in the sentence begins with "modelled using MAHLERAN, and the area over…."

AQ9. Please provide citation for the following references: Cross and Hohenberg (1993), Devitt and Smith (2002), Palutikof et al. (2000), HilleRisLambers et al. (2001), Huxman et al. (2005), Jeltsch et al. (1996, 2010a), Kokkonen et al. (2002), Loik et al. (2004), Minnick and Coffin (1999), Parker et al. (2002), Parsons et al. (1991), Peters (2000), Plackett and Burman (1946), Rietkerk et al. (2004), Sala et al. (1992), Stavi et al. (2009), Todd et al. (1991), Turing (1952), van Palutikof et al. (2000), Walton et al. (2000a).

AQ10. Please confirm the publisher name and location for Fischlin et al. (2007).

AQ11. Please confirm the inserted publisher location for Jeltsch et al. (2010c).

AQ12. Please provide page range for Wainwright Parsons (2002).